

THE JAHN-TELLER EFFECT IN THE ABSORPTION BAND OF ACTIVATED CRYSTALS

BY

GATHUA JOSEPH K.

A THESIS SUBMITTED IN PARTIAL FULFILMENT OF THE REQUIREMENTS FOR THE
DEGREE OF

MASTER OF SCIENCE
DEPARTMENT OF PHYSICS
KENYATTA UNIVERSITY

Gathua, Joseph K.
*The John-teller
effect in the*

1989



92/201080

KENYATTA UNIVERSITY LIBRARY

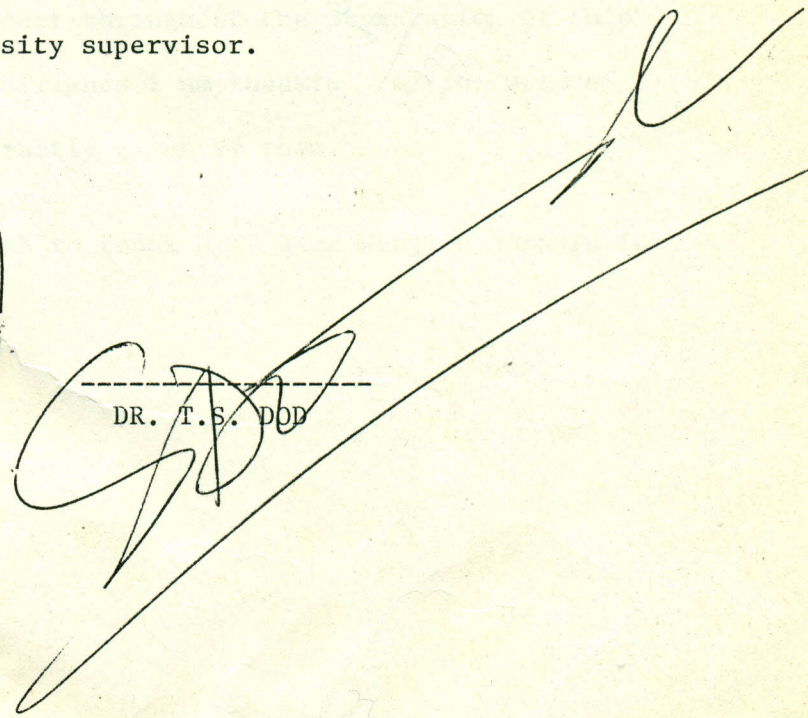
DECLARATION

This thesis is my original work and has not been presented for a degree in any University.



GATHUA JOSEPH K.

This thesis has been submitted for examination with my approval as University supervisor.



DR. T.S. DOE

DEPARTMENT OF PHYSICS

KENYATTA UNIVERSITY

ACKNOWLEDGEMENT

I feel highly indebted to express my sincere thanks and gratitudes to my supervisor Dr. T.S. Dod, for his kindness, commitment and devotion throughout the entire period of preparing this thesis. His constant guidance has been highly acknowledged.

Votes of thanks go to the Chairman Prof. T.J. Odera the Chairman of the Department of Physics for his administrative guidance. Special thanks also go to Mr. F. Koga for helping me in all that was required in computer work. His sacrifice and concern merits appreciation. To Mr. S.K. Wambugu and Mr. P. Wanderi much thanks for proof-reading this thesis. I also thank Miss C.W. Waiganjo for her constant moral support throughout the preparation of this thesis. To all my friends I am thankful for the word of encouragement constantly given by them.

Finally, I wish to thank Miss Jane Wanjiru Bernard for typing this thesis.

CONTENTS

	<u>PAGE</u>
TITLE	i
DECLARATION	ii
ACKNOWLEDGEMENT	iii
TABLE OF CONTENTS	iv
ABSTRACT	1
INTRODUCTION	4
 <u>CHAPTER ONE: THE BAND SHAPE FUNCTION</u>	
1. Hamiltonian of impurity-phonon system	13
2. The transition probability	16
3. Absorption coefficient	18
4. Quantum mechanical representation of the band shape function $F(\Omega)$	21
5. Band shape function for optical transitions between adiabatic states	24
 <u>CHAPTER TWO: MOMENTS OF SPECTRAL BANDS</u>	
6. General formulae of moments of spectral bands	30
7. The electron-phonon interaction Hamiltonian based on Lattice-point model	33
8. Investigation of higher order elementary moments; second and third moments	38
 <u>CHAPTER THREE: MOMENTS OF A \rightarrow T ABSORPTION BAND OF Co^{2+} IN CdF_2 AND CaF_2.</u>	
9. Electron wavefunction of Co^{2+} in CdF_2 and CaF_2	43

	<u>PAGE</u>
10. The electron-phonon interaction	
operator	52
11. The phonon sums	66
i) The Jahn-Teller stabilization	
energy	72
ii) Comparison of theoretical and	
experimental values of Jahn-	
Teller electron-phonon interaction	
parameters.....	76
iii) Energy separation (ΔE) between	
extreme peaks.....	76
DISCUSSION AND CONCLUSION	81
REFERENCES	86

ABSTRACT

With the help of matrix formalism of the method of moments by Perlin and Tsukerblat [1], the Jahn-Teller electron-phonon parameters of $A \rightarrow T$ absorption bands in $\text{CdF}_2:\text{Co}^{2+}$ and $\text{CaF}_2:\text{Co}^{2+}$ crystals have been computed at 78K. These parameters are the second moments ($\langle Q_2 \rangle$), third moments ($\langle Q_3 \rangle$) and the Jahn-Teller stabilization energy (ΔE^{J-T}) associated with the optical absorption bands for the ${}^4A_{2g} \rightarrow {}^4T_{1g}$ (P) and ${}^4A_{2g} \rightarrow {}^4T_{1g}$ (F) transitions in both systems. The third coefficient (δ_3) of the Edgeworth series which expresses the band shape function in terms of moments has also been computed. δ_3 describes the asymmetry deviation of the band shape from the Gaussian form. In calculating these Jahn-Teller electron-phonon parameters, the electron-phonon interaction operator was expressed in lattice-point approximation of first order. The wavefunctions for the $|{}^4A_{2g}\rangle$, $|{}^4T_{1g}$ (P) \rangle , and $|{}^4T_{1g}$ (F) \rangle electronic states of Co^{2+} were expressed in terms of Slater determinants taking into consideration the electron-configuration mixing. The phonon sums which appear in the expressions for the moments and Jahn-Teller stabilization energy were determined in "Extended Brillouin Zone" scheme with a cut off phonon wave vector $\alpha_D = (6\pi^2/V_0)^{1/3}$, where V_0 is the volume of a primitive unit cell. There is a close agreement between the theoretical and experimental values available in the literature.

For the ${}^4A_{2g} \rightarrow {}^4T_{1g}$ (P) absorption band, the theoretical

values for second moment (G_2) at 78K, third moment (G_3) and Jahn-Teller stabilization energy (ΔE^{J-T}) for Co^{2+} in CdF_2 and CaF_2 are G_2 (78K) = $8.9 \times 10^{-3} eV^2$, $G_3 = 1.51 \times 10^{-4} eV^3$, $\Delta E^{J-T} = 0.196 eV$ and G_2 (78K) = $12.1 \times 10^{-3} eV^2$, $G_3 = 3.0 \times 10^{-4} eV^3$, $\Delta E^{J-T} = 0.181 eV$ respectively while the corresponding experimental values are G_2 (78K) = $9.6 \times 10^{-3} eV^2$, $G_3 = 3.12 \times 10^{-4} eV^3$, $\Delta E^{J-T} = 0.23 eV$ and G_2 (78K) = $10.2 \times 10^{-3} eV^2$, $G_3 = 2.86 \times 10^{-4} eV^3$, $\Delta E^{J-T} = 0.223 eV$. For the absorption band arising from the ${}^4A_{2g} \rightarrow {}^4T_{1g}$ (F) the theoretical values are G_2 (78K) = $14.3 \times 10^{-3} eV^2$, $G_3 = 2.44 \times 10^{-4} eV^3$, $\Delta E^{J-T} = 0.3 eV$ for $CdF_2:Co^{2+}$. For $CaF_2:Co^{2+}$ the theoretical values are G_2 (78K) = $19.7 \times 10^{-3} eV^2$, $G_3 = 4.83 \times 10^{-4} eV^3$ and $\Delta E^{J-T} = 0.292 eV$. The experimental values for ΔE^{J-T} are 0.248 eV for $CaF_2:Co^{2+}$ and 0.26 eV for $CdF_2:Co^{2+}$. Further, the third coefficient (γ_3) of Edgeworth series for the ${}^4A_{2g} \rightarrow {}^4T_{1g}$ (P) absorption band has been found to be 0.018 and 0.022 for $CdF_2:Co^{2+}$ and $CaF_2:Co^{2+}$ respectively, while the same is found to be 0.014 and 0.017 for the ${}^4A_{2g} \rightarrow {}^4T_{1g}$ (F) transition in $CdF_2:Co^{2+}$ and $CaF_2:Co^{2+}$ systems respectively. In all these cases $\gamma_3 \ll 1$ which clearly indicates the presence of strong Jahn-Teller lattice interaction. The deviation in agreement varies from 5% to 50% which may be due to the approximations applied e.g. taking into consideration the first nearest neighbour only and expressing the electron-phonon interaction operator in lattice-point approximation of first order.

These findings, however, clearly establish the validity of the lattice-point model for electron phonon- interaction and the

"Extended Brillouin Zone" scheme in calculating the phonon sums to the $\text{CdF}_2:\text{Co}^{2+}$ and $\text{CaF}_2:\text{Co}^{2+}$ crystals and in general to the systems having d-electron deep impurity centres in cubic symmetry.

INTRODUCTION

In crystals, several types of point defects are commonly found including both positive and negative vacancies and interstitial point defects. If trace amounts of a foreign material are introduced into a crystal so as to occupy normal lattice sites, the resulting point defects are termed substitutional impurities which may have large and varied effects on physical and optical properties of the crystal. In general, the optical properties of the impurity or activated crystals which absorb light in the transparency region of the host crystal are quite different from those of pure crystals. The absorption band of impurity crystals consists of a broad band unlike the discrete line spectra in isolated atoms or ions.

Lax[1], Huang Rhays [2] advanced the first theory of light absorption in activated crystals based on adiabatic approximation in the early fifties. In this approximation, both the electrons of the host crystal and those of the impurity centre play the role of fast sub-systems whose states remain invariant when the impurity optical transitions take place. It is assumed in this approximation that any fixed nucleus position corresponds to a stationary electronic states and the nuclear states are determined by the averaged field of the electrons [3]. Many of the optical transitions in electronic systems of impurity crystals involve degeneracy such that the electron - lattice coupling displays the Jahn-Teller (J-T) problem. This is due to the high symmetry

associated with the surroundings of the localized electronic systems in impurity crystals [4].

In the original papers of Jahn and Teller [5], the nuclear displacement is taken to be a quasi-static parameter for the electronic potential energy. The adiabatic potential for the nuclear system belonging to the originally degenerate states exhibits minima away from the minimum of the original symmetry (Jahn-Teller distortion). In this way, the static nuclear configuration lowers its symmetry until the degeneracy is removed. The first calculations of the electronic absorption band shapes for the Jahn-Teller (JT) systems in a semi-classical approximation were conducted by O'Brien [6], Moran [7] and Toyozawa and Inoue [8]. In these systems having degenerate electronic states, besides the totally symmetric coordinate, the non-totally symmetric Jahn-Teller active coordinates are displaced due to electron - lattice interaction. A computer evaluation of the band shapes of the optical transition $A \rightarrow E(e)$ in the above cited papers proved Jahn-Teller interactions to result in a two humped band shape. $E(e)$ is a doubly degenerate electronic state (irreducible representation -E) interacting with a two-fold lattice vibrations (irreducible representation - e) and A is a non-degenerate electronic state. Such a band shape is shown in fig. 1(a). It was a symmetric shape with two humps and a dip at $\Omega = \Omega_0$ where Ω and Ω_0 are the frequency of the incident light and the zero phonon line frequency respectively. $F(\Omega)$ is the band shape function of the absorption band. If one

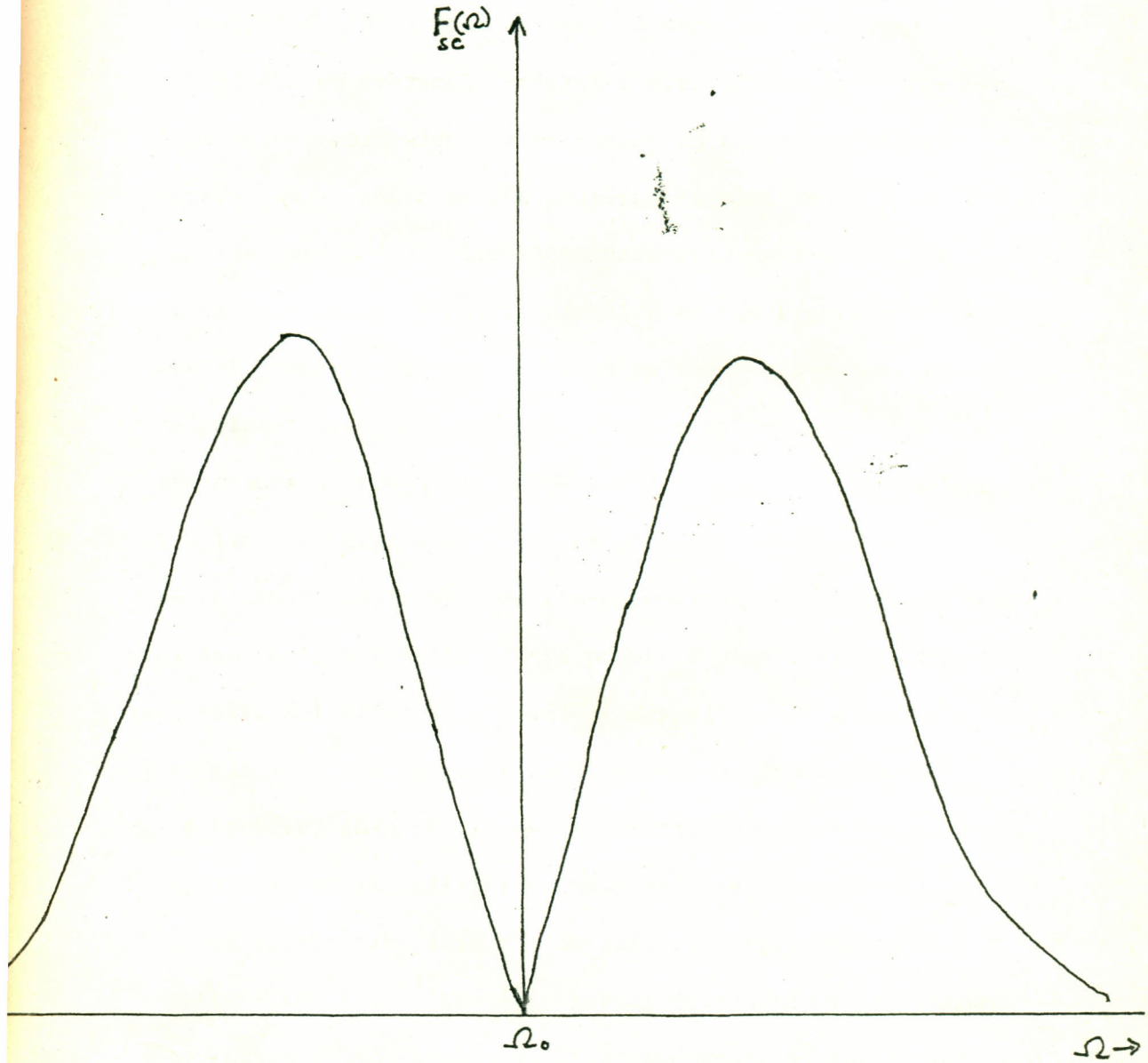


Fig. 1a. Band shape of $A \rightarrow E(e)$ in semiclassical approximation [8].

takes into account that the totally symmetric contribution is non-zero, then the dip of the band shape is smoothed as shown in fig.1(b). Similar results were obtained for transitions to orbitally triplet electronic states. The band shape in this case depends primarily on the relationship between the strength of the coupling of electronic state $\{T\}$ with the lattice vibrations characterized by irreducible representations A, E and T depending on the symmetry of the impurity centre. If the coupling to the E-vibrations is predominant i.e (T-e problem), then no splitting of the $A \rightarrow T$ band occurs although the adiabatic potential of the T state is split. In general, it can be said that in case of the absorption transitions from non-degenerate to degenerate state, the band does not split if the point of degeneracy on the adiabatic potential is a point of actual crossing of the surfaces. If the coupling to T_2 vibration predominates (T-t problem) then the $A \rightarrow T$ absorption band has three humps, the band is split into three components as shown in fig. 2, but the interaction with the totally symmetric vibrations smoothens the band. Cho [9], taking into account the linear interaction of the centre with lattice modes of the A_{1g} , E_g and T_{2g} symmetries made calculations for the triplet structure of the C bands and the doublet structures of the A-bands of S^2 - type centres in alkali halides and deduced that these are due to dynamical Jahn-Teller effect. Fakuda [10] did similar calculations for NaCl and CsCl type crystals and found that the point symmetry of the impurity centre is important in determining the shape of the band.

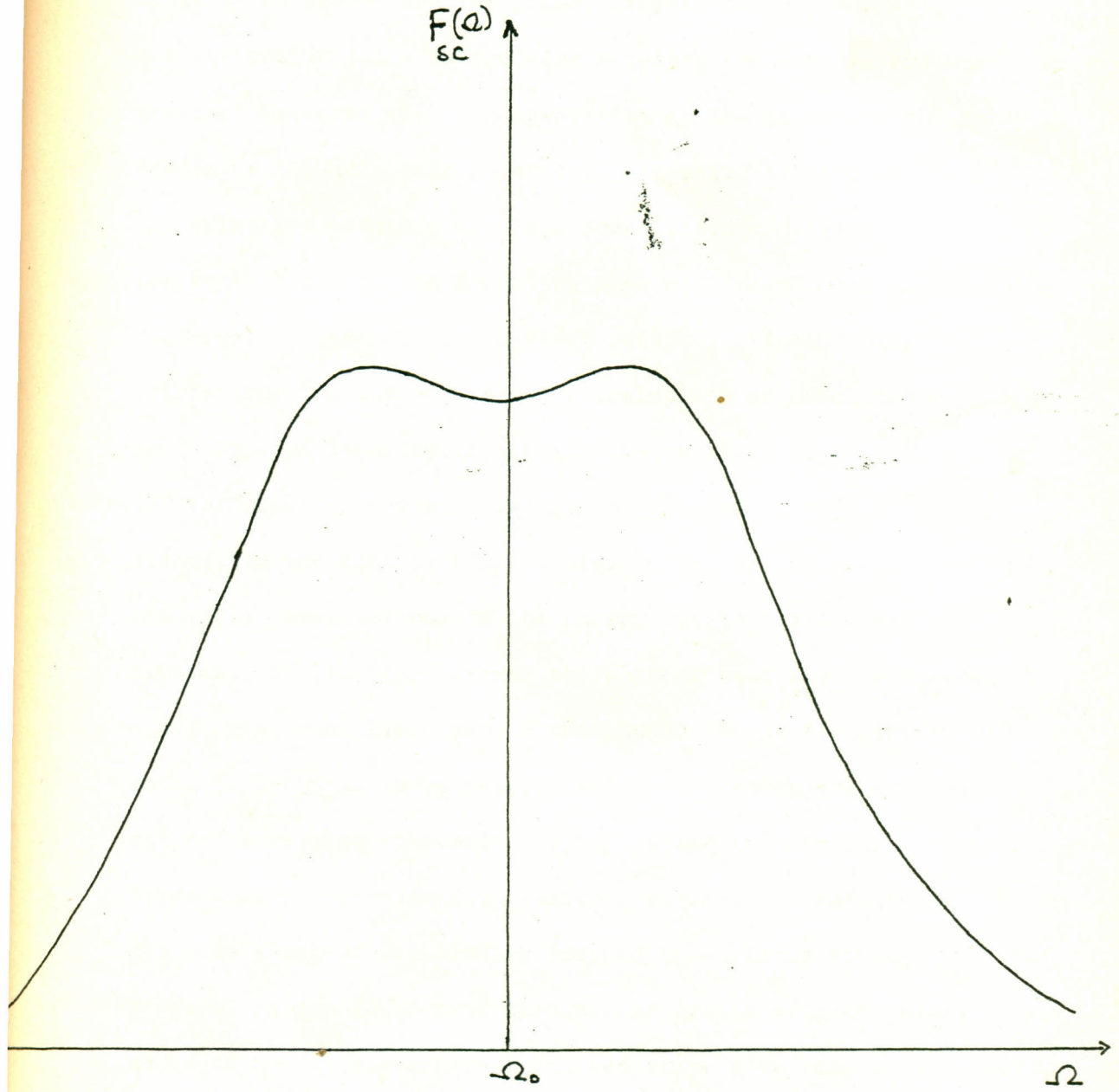


Fig. 1b. Band shape of $A \rightarrow E(a + e)$ in semiclassical approximation [8].

The semi-classical approximation allows the derivation of the band shape in the strong coupling scheme and high temperature limit when the phonon dispersion is taken into account but it fails in the weak coupling and low temperature region. Moreover, for the transition in the intersection region of the adiabatic potential, the validity of this approximation breaks down since some distinct details like the central dip of the $A \rightarrow E(e)$ band and the central peak of $A \rightarrow T(t_2)$ cannot be explained reliably. Today there exists some quantum mechanical calculations of absorption band shape of impurity crystals. The earliest calculation for the absorption band arising from the $A \rightarrow E$ type transition was done by Longuet Higgins et. al. [11]. He used numerical computations of the energy levels for the E-e problem. At low temperatures the optical band for the $A \rightarrow E$ and $E \rightarrow A$ transitions gave a two humped asymmetric curve and a bell-shaped curve respectively. The asymmetry smoothed out on increasing vibronic coupling parameter. Using Frank-Condon approximation, Kamimura et al. [12] calculated the line shape of Jahn-Teller induced transitions at high temperature and found that transitions from a singlet ground state to a nearly degenerate excited state give rise to a broad band. In the other case in which both ground state and excited state are nearly degenerate it gives a very sharp peak. On employing quantum mechanical methods to calculate the intensity and peak position at low temperature in the static limit of Jahn-Teller interaction, the transition proved too weak for the first case to be observed while in the second

case it appeared as a single line. Similar calculations of optical absorption band shapes were done by Koswig et al. [13] for silver halides doped with Cr^{2+} , while Chlopin et al. [14] carried out calculations of band shape in Renner-type systems with strong vibronic coupling.

Canner and Englman [15] applied numerical method to compute the band shape of the transition $A \rightarrow T(t_2)$ and obtained a three humped structural band, these being the consequences of Jahn-Teller effect. The band was presented as a parade of discrete non-broadened lines in the above cited papers and these lines were replaced by Gaussian curve to obtain the envelop. The continuous bands in the crystals however, arise not only due to the broadening of the individual vibronic transitions but mainly from the dispersion of lattice vibrations. Hence, the shape of the band depends on the distribution density of phonons and for this reason the numerical results are more applicable to molecular systems rather than to impurities in crystals. Since the numerical methods take into account only a limited number of excited vibrational levels, the accuracy of such calculations is lost when the electron-phonon interaction is strong.

So far the theoretical computation of band shape function has been possible in some approximations particularly where the Schrodinger equation could be solved, but in fact, the Schrodinger equation cannot be solved due to the coupling of electron and nuclear motions, in particular, for degenerate electronic states. However, with the help of group theoretical analysis, the

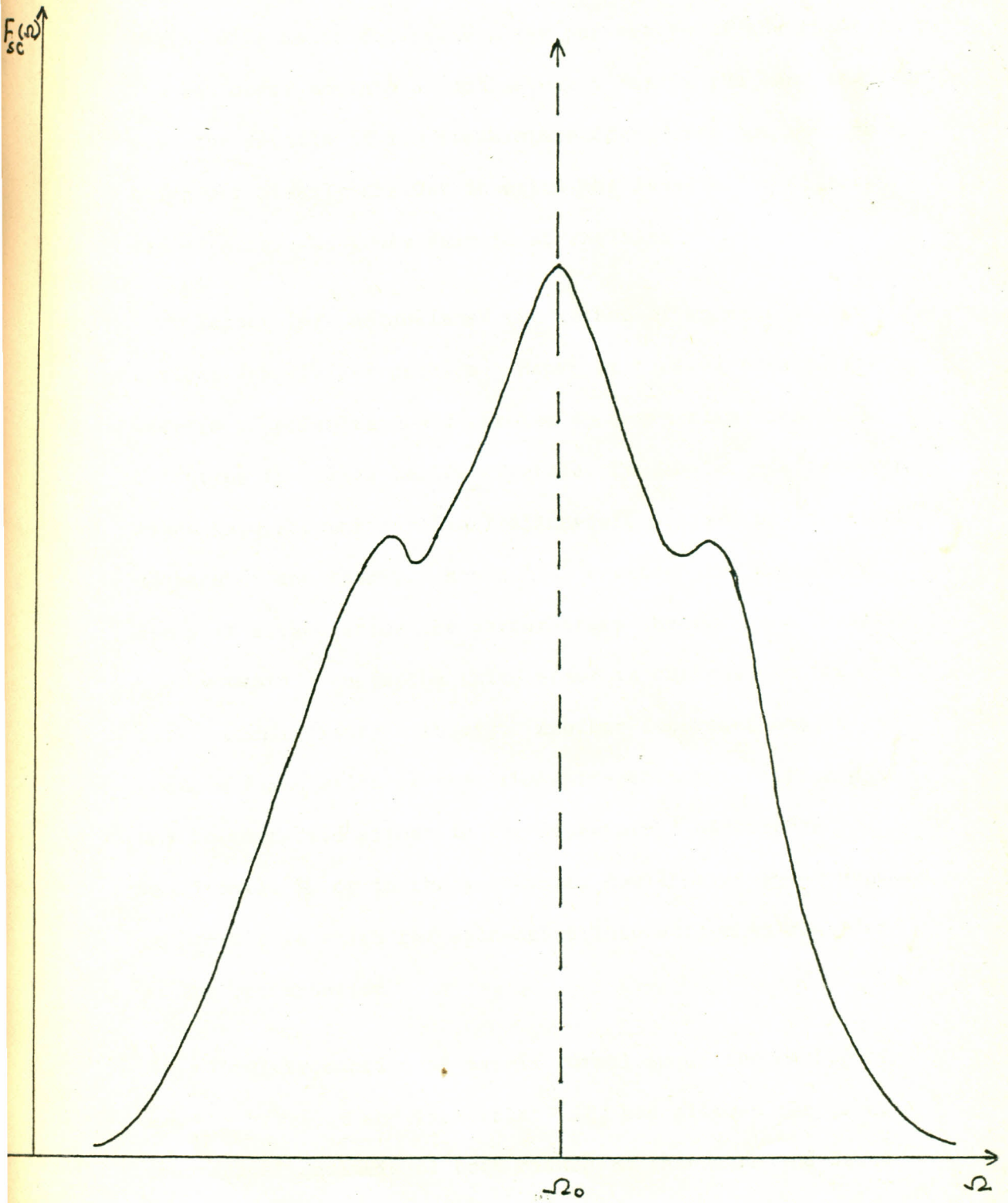


Fig. 2. Absorption band shape of the $A \rightarrow T(t_2)$ electronic transition in semi-classical approximation [8].

moments of the band shape function can be computed accurately, which helps us to determine a few parameters of the theory. The low order moments do not uniquely define the band shape or even the details of its temperature dependence but they do bring out clearly the way in which the Jahn-Teller effect accounts for the gross feature of the band.

Wagner [4] established the method of moments of the optical Jahn-Teller problem. Henry et al. [16] treated the effects of polarization dichroism in conformity with F-centres in alkali halide crystals. The Jahn-Teller effect was taken into account for final electronic states, an important advance of the theory. Honma [17] extended the method by Henry et al. and using the perturbation theory, he calculated the moments upto the third order in contrast to the first order in Henry's theory. Another important aspect in Honma's formulation is that the spin-orbit interaction H_{so} may be contained either in the unperturbed electronic Hamiltonian H_0 or in the perturbing Hamiltonian H_p as opposed to Henry's in which the spin-orbit interaction is regarded as the perturbation.

The introduction of matrix formalism of the method of moments by Perlin and Tsukerblat [18] has allowed the group theoretical analysis of both dichroism phenomena and Jahn-Teller effect for systems with impurity centres having definite point symmetry.

CHAPTER 1

THE BAND SHAPE FUNCTION

1: Hamiltonian of the impurity-phonon system

A pure crystal is composed of an ideal periodic arrangement of atoms, ions or molecules, which possesses a translational symmetry $\vec{R} = n_1 \vec{a}_1 + n_2 \vec{a}_2 + n_3 \vec{a}_3$ extending over the entire volume of the specimen where \vec{a}_i are primitive vectors and n_i the integers. Any deviation from the ideal periodic arrangement of the constituents of the crystal is a lattice imperfection or crystal defects. They are either vacancies at the crystal lattice points, atoms at the interstitial positions or impurities at the lattice sites. A crystal in which foreign material (impurity) has been introduced is called an activated or impurity crystal. The study of such impurities in crystals is of particular importance because they affect both physical and optical properties of the host crystal.

A point defect in a crystal lattice destroys the periodic symmetry and hence the normal modes of vibration are modified from their usual waveform. The changes as would be expected are more pronounced in the vicinity of the defect. Any vibrational property which is probed by the defect itself will be quite different from what is in the perfect lattice. It is therefore essential to make calculations for the modification of the vibrations to interpret any property of a defect, for example, the width and shape of electronic absorption lines or bands [19].

The impurity crystal consists of the impurity centre of definite symmetry, the lattice vibrations of the surrounding and the interaction of impurity electrons with the lattice vibrations. The latter is brought about by the neighbouring atoms which during their vibration, disturb the energy states of the impurity centre. This interaction is referred to as the electron-phonon interaction (EPI) whose Hamiltonian will be of great interest throughout this thesis. In a crystal, the total Hamiltonian is composed of a large number of space and momentum coordinates of all atoms and electrons. But without loss of generality, the Hamiltonian of the electron-phonon system can be constructed using adiabatic-approximation. In this approximation, as was pointed out in the introduction, both the electrons of the host crystal and those of the impurity centre play the role of fast sub-system whose state remains unchanged when the impurity optical transitions take place. Under this assumption the Hamiltonian of the impurity phonon system can be expressed as

$$\hat{H} = \hat{H}_e(\vec{r}) + \hat{H}_{el}(\vec{r}, \vec{q}) + \hat{H}_L(\vec{q}) \dots\dots\dots (1.1)$$

$\hat{H}_e(\vec{r})$ describes the electronic Hamiltonian which includes the total energy of impurity electrons and their interaction energy with the crystal field. $\hat{H}_L(\vec{q})$ is the Hamiltonian of the free vibrations of the host crystal. $\hat{H}_{el}(\vec{r}, \vec{q})$ describes the interaction of the optical electrons of the impurity centre and the lattice vibrations. The appearance of the broad optical bands, associated with Jahn-Teller effect and temperature shift among others are some of the well known

optical manifestations of this electron-phonon interactions.

If $V(\vec{r})$ is the potential of the electron due to the nucleus of the impurity centre plus the potential due to the surrounding assuming that the lattice points are at rest, then one can write

$$\hat{H}_e(\vec{r}) = -\frac{\hbar^2}{2M} \nabla^2 + \hat{V}(\vec{r}) \quad \dots\dots\dots (1.2)$$

where M is the mass of lattice point.

If \hat{P} and ω are the momentum operator and the angular frequency of harmonic oscillator respectively, and R the displacement of the lattice point from the equilibrium position, then the Hamiltonian of lattice vibration in harmonic oscillator approximation can be expressed as

$$\hat{H}_L(\vec{r}) = \frac{\hat{P}^2}{2M} + M\omega^2 R^2 \quad \dots\dots\dots (1.3)$$

In terms of normal coordinates $q_{\vec{x}}$ of lattice vibration eq. (1.3) can be written as

$$\hat{H}_L(\vec{r}) = \sum_{\vec{x}} \hbar\omega_{\vec{x}} \left(q_{\vec{x}}^2 - \frac{\partial^2}{\partial q_{\vec{x}}^2} \right) \quad \dots\dots\dots (1.4)$$

where \vec{x} is the wave vector of the lattice-vibrations. In the language of second quantization, by introducing the so called the creation and annihilation phonon-operators viz $\hat{C}_{\vec{x}}^+$ and $\hat{C}_{\vec{x}}$, respectively, the Hamiltonian for lattice vibrations eq. (1.4) can be rewritten as [20]:

$$\hat{H}_L = \sum_{\vec{x}} \hbar\omega_{\vec{x}} \left(\hat{C}_{\vec{x}}^+ \hat{C}_{\vec{x}} + \frac{1}{2} \right) \quad \dots\dots\dots (1.5)$$

In the first order (linear) approximation with respect to $\hat{Q}_{\vec{x}}$ the electron-phonon interaction Hamiltonian can be written as.

$$\hat{H}_{el} = \sum_{\vec{x}} \hat{V}_{\vec{x}}(\vec{r}) \hat{Q}_{\vec{x}}, \dots\dots\dots (1.6)$$

where $\hat{V}_{\vec{x}}$ is the electronic operator.

2: The transition probability

Transitions which are accompanied by a change in electron dipole moments are called electric dipole moments transitions while those accompanied by a change in magnetic dipole moments are called magnetic dipole moment transitions.

The electric dipole moment transition has the highest probability to occur and so the transition probability will be discussed with respect to this transition.

If a ray of light is incident on a crystal plane, the impurity atom absorbs a photon and transition of electron may take place from a certain initial state $|i\rangle$ to a final state $|f\rangle$. The transition probability from the initial state $|i\rangle$ to the final state $|f\rangle$ is given by.

$$\omega_{i \rightarrow f} = \frac{|d_{fi}|^2}{\hbar^2} |\mathcal{E}(\omega)|^2, \dots\dots\dots (2.1)$$

where d_{fi} is defined as

$$d_{fi} = \langle f | \hat{d} | i \rangle \dots\dots\dots (2.2)$$

which is the matrix element of the electric dipole moment between the final state $|f\rangle$ and initial state $|i\rangle$ and

$$\vec{d} = -e \cdot \vec{r} \dots\dots\dots (2.3)$$

is the electric dipole moment of electron. If $\mathcal{E}(\Omega)$ is the Fourier component of the electric field of light waves such that,

$$\mathcal{E}(\Omega) = \int \mathcal{E}(t) e^{i\Omega t} dt \dots\dots\dots (2.4)$$

and Ω is the angular frequency of light waves, then on performing the reverse operation, eq. (2.4) becomes

$$\mathcal{E}(t) = \frac{1}{2\pi} \int \mathcal{E}(\Omega) e^{-i\Omega t} d\Omega \dots\dots\dots (2.5)$$

To find the expression for ω_{if} in terms of spectral density of radiation, we use the conventional quantum electrodynamic methods. In a dispersionless medium of permittivity ϵ and refractive index n , the Poyntings vector $S(t)$ is given by

$$S(t) = \frac{3\epsilon c}{4\pi n} |\mathcal{E}(t)|^2 \dots\dots\dots (2.6)$$

where c is velocity of light.

Using the Fourier component of \mathcal{E} eq. (2.5), eq. (2.6) becomes

$$S(t) = \frac{3nc}{4\pi} \cdot \frac{1}{(2\pi)^2} \iint \mathcal{E}(\Omega) \mathcal{E}^*(\Omega') e^{-i(\Omega - \Omega')t} d\Omega d\Omega' \dots\dots\dots (2.7)$$

With the help of delta function

$$\frac{1}{2\lambda} \int e^{i(\Omega - \Omega')t} dt = \delta(\Omega - \Omega') \dots\dots\dots (2.8)$$

which is non-zero only when $\Omega = \Omega'$, the energy of the light wave W , falling on a unit area of a crystal can be written as

$$W = \int s(t) dt = \frac{3nc}{8\lambda^2} \int |\mathcal{E}(\Omega)|^2 d\Omega \dots\dots\dots (2.9)$$

which can be expressed as

$$W = \int W(\Omega) d\Omega \dots\dots\dots (2.10)$$

such that

$$W(\Omega) = \frac{3nc}{8\lambda^2} |\mathcal{E}(\Omega)|^2 \dots\dots\dots (2.11)$$

where $W(\Omega)$ is called the spectral density of the radiation. Using eq. (2.11) the transition probability, eq. (2.1) can be written as

$$\omega_{i \rightarrow f} = \frac{8\pi^2}{3nc\hbar^2} |d_{fi}|^2 W(\Omega_{if}) \dots\dots\dots (2.12)$$

Ω_{if} is Bohr frequency of the $i \rightarrow f$ transition.

3: The absorption coefficient

Let us consider the emission flow of spectral density $W(\Omega)$ defined by eq.(2.11) propagating along the Z-direction of the crystal. Due to light absorption the attenuation of the

intensity in an interval dz will be defined by the equation

$$\frac{dW(\Omega, z)}{W(\Omega, z)} = -K(\Omega) dz \quad \dots\dots\dots (3.1)$$

where $K(\Omega)$ is the absorption coefficient for the frequency Ω of the light absorbed. $dW(\Omega, z)$ is the change in spectral density in a distance dz . We take dw as the energy absorbed by the medium per unit area through a depth dz . i.e the energy absorbed in a volume $1 \text{ unit}^2 \times dz$. On integration, eq. (3.1) yields

$$W(\Omega, z) = W(\Omega, 0) e^{-K(\Omega)z} \quad \dots\dots\dots (3.2)$$

If N_c is the concentration of absorbing centres per unit volume and each centre absorbs energy given by $\hbar\Omega_{if}$, then the total energy absorbed by all the centres in a volume $(1 \text{ unit}^2 \times dz)$ will be equal to

$$N_c (1 \text{ unit}^2 \times dz) \hbar\Omega_{if} \omega_{if} = N_c dz \hbar\Omega_{if} \omega_{if} = K(\Omega) W(\Omega, z) dz \quad \dots\dots\dots (3.3)$$

Now, using eq. (2.12), eq. (3.3) becomes

$$N_c \hbar\Omega_{if} \frac{8\pi^2}{3nc} \frac{|d_{fi}|^2}{\hbar^2} W(\Omega, z) dz = K(\Omega_{if}) W(\Omega_{if}) dz \quad \dots\dots\dots (3.4)$$

from which we get

$$K_{if}(\Omega_{if}) = \frac{8\pi^2 N_c}{3\hbar nc} \Omega_{if} |d_{fi}|^2 \quad \dots\dots\dots (3.5)$$

Eq. (3.5) defines the absorption coefficient for the single transition between the two states $i \rightarrow f$. The total coefficient of absorption is obtained by summing over the final states and taking the average over the initial states, which is in thermal equilibrium. If P_i is the occupation probability of the initial state, then

$$K(\Omega) = \sum_{if} P_i K_{if}(\Omega_{if}) \dots\dots\dots (3.6)$$

where P_i is defined as [23]:

$$P_i = \frac{e^{-E_i/k_B T}}{Z} \dots\dots\dots (3.7)$$

Z is the partition function for all the initial states and is given by

$$Z = \sum_i e^{-E_i/k_B T} \dots\dots\dots (3.8)$$

Eq. (3.6) can as well be put in the form,

$$K(\Omega) = \sum_{if} P_i \int K_{if}(\Omega) \delta(\Omega - \Omega_{if}) d\Omega \dots\dots\dots (3.9)$$

In assigning the occupation probability P_i to the initial state, we assumed that the final state is not populated.

Writing

$$K(\Omega) = \int \mathcal{K}(\Omega) d\Omega \dots\dots\dots (3.10)$$

where $K(\omega)$ is the spectral density of the absorption coefficient, $K(\omega)$ can be written as

$$K(\omega) = \sum_{if} p_i K_{if}(\omega) \delta(\omega - \omega_{if}) \dots\dots\dots (3.11)$$

Substituting eq. (3.5), into eq. (3.11) $K(\omega)$ becomes

$$K(\omega) = \frac{8\pi^2 N_c \Omega}{3nc\hbar} \sum_{if} p_i |d_{fi}|^2 \delta(\omega - \omega_{if}) \dots\dots (3.12)$$

or

$$K(\omega) = \frac{8\pi^2 N_c \Omega}{3nc\hbar} F(\omega) \dots\dots\dots (3.13)$$

where

$$F(\omega) = \sum_{if} p_i |d_{fi}|^2 \delta(\omega - \omega_{if}) \dots\dots\dots (3.14)$$

$F(\omega)$ is called the band-shape function of the electric dipole transition.

4: Quantum mechanical representation of $F(\omega)$

The expression of the band shape function eq. (3.14) suggests that one of the appropriate ways of solving for the function is by use of the time-correlation function.

By definition we have,

$$\delta(\omega - \omega_{if}) = \frac{1}{2\pi} \int e^{i(\omega - \omega_{if})t} dt \dots\dots\dots (4.1)$$

such that eq. (3.14) becomes

$$F(\Omega) = \frac{1}{2\pi} \int_{-\infty}^{\infty} \sum_{if} p_i |\langle f | \hat{d} | i \rangle|^2 e^{i(\Omega - \Omega_{if})t} dt \dots (4.2)$$

and writing

$$I(t) = \sum_{if} p_i |\langle f | \hat{d} | i \rangle|^2 e^{-i\Omega_{if}t} \dots (4.3)$$

$F(\Omega)$ can be written as

$$F(\Omega) = \frac{1}{2\pi} \int_{-\infty}^{\infty} e^{i\Omega t} I(t) dt \dots (4.4)$$

Using eq. (3.7), eq. (4.3) becomes,

$$I(t) = \sum_{if} \frac{e^{-E_i/k_B T}}{Z} |\langle f | \hat{d} | i \rangle|^2 e^{-i\Omega_{if}t} \dots (4.5)$$

Since $\Omega_{if} = \frac{-(E_f - E_i)}{\hbar}$, (4.6)

eq. (4.5) can be expressed as

$$I(t) = \frac{1}{Z} \sum_{if} e^{-E_i/k_B T} |\langle f | \hat{d} | i \rangle|^2 e^{\frac{-i(E_f - E_i)t}{\hbar}} \dots (4.7)$$

Setting $\lambda = 1/k_B T$, then $I(t)$ can be expressed as

$$I(t) = \frac{1}{Z} \sum_{if} e^{-\lambda E_i} \langle i | \hat{d}^\dagger | f \rangle \langle f | \hat{d} | i \rangle e^{\frac{-i(E_f - E_i)t}{\hbar}} \dots (4.8)$$

Since E_i is an eigenvalue of \hat{H} one can express eq. (4.8) equally well in terms of the Hamiltonian by performing the

reverse operation such that

$$I(t) = \frac{1}{Z} \sum_{if} \langle i | e^{-\lambda \hat{H}} e^{\frac{i\hat{H}t}{\hbar}} \hat{d}^+ e^{-\frac{i\hat{H}t}{\hbar}} | f \rangle \langle f | \hat{d} | i \rangle \dots (4.9)$$

Now writing

$$\hat{d}^+(t) = e^{\frac{i\hat{H}t}{\hbar}} \hat{d}^+ e^{-\frac{i\hat{H}t}{\hbar}} \dots (4.10)$$

eq. (4.9) becomes

$$I(t) = \frac{1}{Z} \sum_{if} \langle i | e^{-\lambda \hat{H}} \hat{d}^+(t) | f \rangle \langle f | \hat{d} | i \rangle \dots (4.11)$$

Taking the average over the initial thermodynamic equilibrium state, $I(t)$ is written as

$$I(t) = \frac{1}{Z} \sum_i \langle i | e^{-\lambda \hat{H}} \hat{d}^+(t) \hat{d} | i \rangle \dots (4.12)$$

which can be further expressed as

$$I(t) = \frac{1}{Z} \text{Tr} [e^{-\lambda \hat{H}} \hat{d}^+(t) \hat{d}] \dots (4.13)$$

For a given operator \hat{P} , the quantum statistical average is given by [22].

$$\langle \hat{P} \rangle_s = \frac{1}{Z} \text{Tr} (e^{-\lambda \hat{H}} \hat{P}) \dots (4.14)$$

This allows us to write the R.H.S of eq. (4.13) as a quantum statistical average of the operator $[\hat{d}^+(t) \hat{d}]$ such that

it becomes

$$I(t) = \langle \hat{d}^+(t) \hat{d} \rangle_s \dots\dots\dots (4.15)$$

Finally, using eq. (4.15) the band shape function $F(\omega)$ can be expressed as

$$F(\omega) = \frac{1}{2\pi} \int_{-\infty}^{\infty} \langle \hat{d}^+(t) \hat{d} \rangle_s e^{i\omega t} dt \dots\dots(4.16)$$

This is the quantum mechanical representation of the band shape function. In deriving this equation an assumption has been made that the final state is empty and also the $f \rightarrow i$ transitions have been ignored. If this is taken into account the function will be given by,

$$F(\omega) = \frac{1}{2\pi} (1 - e^{-\lambda\hbar\omega}) \int_{-\infty}^{\infty} e^{i\omega t} \langle \hat{d}(t) \hat{d} \rangle_s dt \dots\dots (4.17)$$

But in the optical region $\hbar\omega \gg k_B T$ such that the term $e^{-\lambda\hbar\omega}$ can be ignored and to a good approximation eq. (4.16) holds true.

5: Band shape function for optical transitions between adiabatic states.

In this section, the band shape function is expressed for optical transitions between adiabatic states with special attention paid to transitions from a non-degenerate to a degenerate state, i.e. $A \rightarrow T$ transition. It is assumed that the initial electron-vibrational state $|i\rangle$ is adiabatic. This is to mean that the internal and external non-adiabaticities

are negligible and so not considered. For external non-adiabaticity of initial state to be negligible, the energy gap between this level and others should be large as compared to the phonon energy. This means that if E_i and E_f are the energies of the initial and final states and $\hbar\omega$ is the typical phonon energy, then

$$E_f - E_i \gg \hbar\omega \quad \dots\dots\dots (5.1)$$

The internal non-adiabaticity condition is trivially satisfied for a non-degenerate electronic state. If $|i\rangle$ and $|f\rangle$ are the initial and final eigenfunctions of the initial Hamiltonian \hat{H}^i , having the adiabatic part of H_{el} , and because of the unitary invariance of the trace operator, one can write the shape function given by eq. (4.17) as

$$F(\Omega) = \frac{1}{2\pi\lambda Z} \sum_{fi} \int_{-\infty}^{\infty} e^{i\Omega t} \langle i | e^{-\lambda \hat{H}^i} e^{\frac{i\hat{H}^i t}{\hbar}} \hat{d}^{\dagger} e^{-\frac{i\hat{H}^i t}{\hbar}} | f \rangle \langle f | \hat{d} | i \rangle \dots\dots (5.2)$$

The operator \hat{d} operates on electron coordinates and so remains unchanged. Since the initial state is assumed to be adiabatic, and if $|A\rangle$ is the initial electronic wavefunction, then the adiabatic approximation allows one to write the wavefunction of the initial state as

$$|i\rangle = |A\rangle \prod_{\alpha} |n_{\alpha}\rangle, \dots\dots\dots (5.3)$$

where n_{α} are the phonon occupation numbers. Taking $\hbar\Omega_i$ to be the eigenvalue of the electronic Hamiltonian and following

the said approximation, we obtain,

$$Z = \sum_i \langle i | e^{-\lambda H} | i \rangle = Z_L e^{-\lambda \hbar \Omega_i} \dots\dots\dots (5.4)$$

where Z_L is the phonon partition function defined by the equation.

$$Z_L = \prod_{\vec{\alpha}} \left(2 \sinh \frac{\lambda \hbar \omega_{\vec{\alpha}}}{2} \right)^{-1} \dots\dots\dots (5.5)$$

Now, if $|f_0\rangle$ and $|f\rangle$ are the exact eigenfunctions of the Hamiltonian H_0^i (where $H_0^i = H_e + H_L$) and H^i respectively, then the wavefunction $|f_0\rangle$ can be expressed in adiabatic approximation as

$$|f_0\rangle = |\Gamma_f \gamma_f\rangle \prod_{\vec{\alpha}} |n_{\vec{\alpha}}^i\rangle \dots\dots\dots (5.6)$$

The wavefunction $|\Gamma_f \gamma_f\rangle$ of the "non-self consistent" or the Frank-Condon excited electronic state should be computed at a frozen nuclear configuration corresponding to its equilibrium position in the initial electronic state.

With the help of completeness condition of the phonon wavefunction,

$$\sum_{\vec{\alpha}} |n_{\vec{\alpha}}\rangle \langle n_{\vec{\alpha}}| = 1 \dots\dots\dots (5.7)$$

and the spectroscopic stability condition,

$$\sum_f |f\rangle \langle f| = \sum_{f_0} |f_0\rangle \langle f_0| \dots\dots\dots (5.8)$$

the band shape function given by eq. (5.2) is rewritten as

$$F(\omega) = \frac{1}{2\lambda} A_V(A) \sum_{\Gamma_f} \int_{-\infty}^{\infty} dt e^{i(\omega - \omega_f)t} \langle\langle A | e^{\frac{i\hat{H}_t}{\hbar}} \hat{a}^\dagger | \Gamma_f \rangle\rangle \langle \Gamma_f | e^{-\frac{i\hat{H}t}{\hbar}} \hat{a} | A \rangle \dots\dots\dots (5.9)$$

where $\langle \dots \rangle_L$ denotes the phonon average.

We now introduce the evolution operator $\hat{U}_i(t)$ which is defined by the relation

$$\exp(-i\hat{H}^i t/\hbar) = \exp[-i/\hbar (\hat{H}_e + \hat{H}_L)t] \hat{U}_i(t) \dots\dots (5.10)$$

The evolution operator satisfies the differential equation

$$i\hbar \frac{d\hat{U}_i}{dt} = \hat{H}_{eL}(t) \hat{U}_i(t) \dots\dots\dots (5.11)$$

whose solution takes the form,

$$\hat{U}_i(t) = T \exp \left[-i/\hbar \int_0^t \hat{H}_{eL}^i(t_1) dt_1 \right] \dots\dots\dots (5.12)$$

where T is the time ordering operator arranging the time-dependent factors $\hat{H}_{eL}^i(t_1), \hat{H}_{eL}^i(t_2) \dots\dots$ in chronological order $t_1 > t_2 \dots\dots$. $\hat{H}_{eL}(t)$ is the electron-phonon Hamiltonian operator defined by the equation

$$\hat{H}_{eL}(t) = e^{\frac{i\hat{H}_0 t}{\hbar}} \hat{H}_{eL} e^{-\frac{i\hat{H}_0 t}{\hbar}} \dots\dots\dots (5.13)$$

Substituting eq. (5.10) into eq.(5.9) the expression for the band shape function becomes

$$F(\Omega) = \frac{1}{2\pi} A_V(A) \sum_{\Gamma_f \gamma_f} \sum_{\Gamma_i \gamma_i} \int_{-\infty}^{\infty} dt e^{i(\Omega - \Omega_{fi})t} \langle A | \hat{d}^+ | \Gamma_f \gamma_f \rangle \langle \Gamma_i \gamma_i | \hat{U}_i(t) | \Gamma_i \gamma_i \rangle \times \langle \Gamma_i \gamma_i | \hat{d} | A \rangle \dots (5.14)$$

where

$$\Omega_{fi} = \Omega_f - \Omega_i = \frac{E_f - E_i}{\hbar} \dots\dots\dots (5.15)$$

is the frequency of the Frank-Condon transition.

If the initial state is non-degenerate, then the operator

\hat{d} can be represented as the one column matrix with elements $\langle A | \hat{d} | \Gamma_i \gamma_i \rangle$ and $\langle \Gamma_f \gamma_f | \hat{U} | \Gamma_i \gamma_i \rangle$ as a square matrix such that eq. (5.14) can be rewritten as

$$F_\eta(\Omega) = \frac{1}{2\pi} \int_{-\infty}^{\infty} dt e^{i\Omega t} e^{-i\Omega_{fi}t} \langle \hat{d}_\eta^+ \hat{U}(t) \hat{d}_\eta \rangle_L \dots\dots (5.16)$$

where η is the index of polarization of light. Eq. (5.16) can be further expressed as

$$F_\eta(\Omega) = \frac{1}{2\pi} \int_{-\infty}^{\infty} dt e^{i\Omega t} \hat{d}_\eta^+ e^{-\frac{i\hat{H}_e t}{\hbar}} \langle \hat{U}(t) \rangle_L \hat{d}_\eta \dots\dots (5.17)$$

If $\hbar\Omega_0$ is the centre of gravity of the excited levels and \hat{W} the perturbation acting on the system, then

$$\hat{H}_e = \hbar(\Omega_0 \hat{I} + \hat{W}) \quad \dots\dots\dots (5.18)$$

This perturbation describes the splitting of the final electronic states. It involves internal interactions such as spin-orbital, static crystal field as well as interaction with external non-magnetic fields (electric and stress). The perturbation $\hbar\hat{W}$ is assumed to be small compared to the energy gap between the set of excited states forming the band and other excited levels and it just splits the excited level. The inter-multiplet vibronic mixing as suggested by eq. (5.1) is assumed to be non-existent. Finally the band shape functions can be written in the form

$$F_{\eta}(\Omega) = \frac{1}{2\pi} \int_{-\infty}^{\infty} dt e^{i(\Omega - \Omega_0)t} \langle A | \hat{d}_{\eta}^{\dagger} e^{-i\hat{W}t} \langle \hat{U}(t) \rangle \hat{d}_{\eta} | A \rangle \dots (5.19)$$

This expression for band shape function will be used in the next chapter to get the exact expressions for the moments.

CHAPTER 11

MOMENTS OF SPECTRAL BANDS

6: General formulae of moments of spectral bands

For degenerate electronic states of the phonon-impurity systems, the exact analytical derivation of the optical bands is not possible for Jahn-Teller centres. However, the exact computation of moments of absorption spectrum is realizable for a sufficiently real model of the impurity centre [16]. Because of their integral characteristic, the moments of spectral bands can be computed without resorting to solutions of Schrodinger equations. The analytical expression for the spectral moments has been derived up to the third order using the perturbation method [17].

The general definitions of moments of spectral distributions $F(\Omega)$ are given as below:

The zeroth moment (band intensity) is defined as

$$\langle \Omega_0 \rangle = \int F(\Omega) d\Omega \dots\dots\dots (6.1)$$

The first moment (centre of gravity) is defined by

$$\langle \bar{\Omega} \rangle = \frac{1}{\langle \Omega_0 \rangle} \int \Omega F(\Omega) d\Omega \dots\dots\dots (6.2)$$

The second moment which determines the half band width is given by

$$\langle \Omega_2 \rangle = \frac{1}{\langle \Omega_0 \rangle} \int \Omega^2 F(\Omega) d\Omega \dots\dots\dots (6.3)$$

and the third moment which determines the asymmetry of the curve is given by

$$\langle \Omega_3 \rangle = \frac{1}{\langle \Omega_0 \rangle} \int \Omega^3 F(\Omega) d\Omega \dots\dots\dots (6.4)$$

The normalized m^{th} order moment is given by

$$\langle \Omega_m \rangle = \frac{1}{\langle \Omega_0 \rangle} \int \Omega^m F(\Omega) d\Omega \dots\dots\dots (6.5)$$

But the m^{th} order normalized moment measured from the centre of gravity is defined as

$$\langle \Omega_m \rangle = \frac{1}{\langle \Omega_0 \rangle} \int (\Omega - \bar{\Omega})^m F(\Omega) d\Omega \dots\dots (6.6)$$

The integration extends over the range $-\infty \leq \Omega \leq \infty$. Using eq. (5.19) for the band shape function and eq. (6.1) the following expression for the zeroth moment is obtained

$$\langle \Omega_0 \rangle_{\eta} = \sum_{r\gamma} \langle A | \hat{d}_{\eta}^+ | r\gamma \rangle \langle r\gamma | \hat{d}_{\eta} | A \rangle \dots\dots (6.7)$$

and in operator form this is written as

$$\langle \Omega_0 \rangle_{\eta} = \hat{d}_{\eta}^+ \hat{d}_{\eta} \dots\dots\dots (6.8)$$

This equation shows that the zeroth moment is perturbation independent and so is the band intensity. This result justifies why eq. (5.8) is called the 'spectroscopic stability principle'.

Making use of the relation,

$$\frac{1}{2\pi} \int_{-\infty}^{\infty} \Omega e^{i\Omega t} d\Omega = -i \frac{d}{dt} \delta(t) \dots\dots\dots (6.9)$$

the expression for the first moment becomes

$$\langle \bar{\Omega} \rangle_{\eta} = \langle \Omega_0 \rangle + \frac{1}{\langle \Omega_0 \rangle_{\eta}} \langle \hat{d}_{\eta}^{\dagger} \hat{W} \hat{d}_{\eta} \rangle \dots\dots (6.10)$$

\hat{W} is the perturbation and eq.(6.10) is valid for linear electron-phonon interaction. Under this circumstance, i.e when $\langle \dot{U}(0) \rangle = 0$, the first moment does not depend on temperature and does not involve the phonon correction. It is through higher-order terms in the expansion of H_{el} in nuclear displacements that the corrections of this kind appear.

Following similar transformations, the m^{th} normalized and centralized moment of the absorption band due to transitions arising from a non-degenerate ground state to the excited multiplet takes the form

$$\langle \Omega^m \rangle_{\eta} = \sum_{k=0}^m \binom{m}{k} \hat{d}_{\eta}^{\dagger} (\hat{W} - \Delta \langle \bar{\Omega} \rangle_{\eta} \hat{I})^{m-k} \hat{\sigma}_k \hat{d}_{\eta} \dots\dots (6.11)$$

where $\Delta \langle \bar{\Omega} \rangle_{\eta}$ is given by

$$\Delta \langle \bar{\Omega} \rangle_{\eta} = \frac{1}{\langle \Omega_0 \rangle} \langle \hat{d}_{\eta}^{\dagger} \hat{W} \hat{d}_{\eta} \rangle \dots\dots\dots (6.12)$$

$\binom{m}{k}$ are the binomial coefficients, \hat{d}_{η} is a one-column matrix of the electric dipole moment, and $\Delta \langle \bar{\Omega} \rangle_{\eta}$ is the field

induced shift of the first moment. The matrix \hat{G}_k , called elementary moment is given by the equation,

$$\hat{G}_k = (-i)^k \left\langle \frac{d^k \hat{U}(t)}{dt^k} \Big|_{t=0} \right\rangle \dots\dots\dots (6.13)$$

where $U(t)$, the evolution operator is defined by

$$\hat{U}(t) = T \exp \left[i/\hbar \int_0^t \hat{H}_{eL}(t_1) dt_1 \right] \dots\dots\dots (6.14)$$

The matrices \hat{G}_k determine the effect of electron-phonon interaction on the band shape and its temperature dependence.

7: The Electron-phonon Interaction Hamiltonian based on the lattice-point model

The expression for the electron-phonon interaction Hamiltonian (H_{eL}) and electronic states in the crystal are derived in lattice-point model. In the lattice-point model, ions or atoms are situated at the lattice sites and the impurity centre observe some crystal symmetry. There are two types of impurity centres. In the first case of impurity centres, the effective radius of the electronic state is greater than the crystal lattice constant. In this case as the electron moves in the crystal, the potential of the lattice forms a system referred to as a polaron. Such polarons have been observed to exist in crystals. In the second case the effective radius of electronic state of the impurity centre is less than the lattice constant, a case which is true in deep impurity centre electrons and especially for p, d and f

KENYATA UNIVERSITY

electrons of impurity ions.

The interaction of the optical electrons of the impurity centre with lattice vibrations of the surrounding lattice atoms or ions is due to the modulation of crystal field by the lattice vibrations.

If \vec{R}_{α_0} is the equilibrium position of the α^{th} lattice point, \vec{R}_α is the new position of the same after displacement, the displacement of this lattice point from the equilibrium position, $\Delta\vec{R}_\alpha$ can be expressed as

$$\Delta\vec{R}_\alpha = \vec{R}_\alpha - \vec{R}_{\alpha_0} \dots\dots\dots (7.1)$$

$|\Delta R_\alpha|$ is small compared to the lattice constant. Now $\hat{W}(\vec{r}_k, \vec{R}_\alpha)$, the electrostatic potential energy of the optical electrons with the ligands of the surrounding is expressed as

$$\hat{W}(\vec{r}_k, \vec{R}_\alpha) = \sum_{\alpha, k} \frac{1}{4\pi\epsilon_0} \frac{ee^*}{|\vec{r}_k - \vec{R}_\alpha|} \dots\dots\dots (7.2)$$

where \vec{r}_k is the position of the k^{th} electron, e^* the effective charge of the lattice ion, ϵ_0 the permittivity of the vacuum. The summation is carried over all the ions of the surroundings and the electrons of the impurity centre. The electron-phonon interaction operator in the first order displacement is written as [18],

$$\hat{H}_{eL} = \sum_{\alpha, k} \frac{\partial \hat{W}(\vec{r}_k \dots \vec{R}_\alpha)}{\partial \vec{R}_\alpha} \Big|_{\vec{R}_\alpha = \vec{R}_{\alpha 0}}, \Delta \vec{R}_\alpha \dots \dots \dots (7.3)$$

which with the help of eq. (7.2) is written as

$$\hat{H}_{eL} = \sum_{\alpha, k} \nabla_\alpha \frac{e e^*}{4\pi\epsilon_0 |\vec{r}_k - \vec{R}_\alpha|} \Big|_{\vec{R}_\alpha = \vec{R}_{\alpha 0}}, \Delta \vec{R}_\alpha \dots \dots \dots (7.4)$$

With the help of group theory the cartesian displacements $\Delta \vec{R}_\alpha$ can be transformed into the so called symmetrized displacements $\vec{Q}_{\bar{\Gamma}\bar{\gamma}}$ using the transformation [23]

$$\vec{Q}_{\bar{\Gamma}\bar{\gamma}} = \hat{P}_{\bar{\Gamma}\bar{\gamma}}^{(\bar{\Gamma})} \Delta \vec{R}_\alpha \dots \dots \dots (7.5)$$

where $\hat{P}_{\bar{\Gamma}\bar{\gamma}}^{(\bar{\Gamma})}$ is the projection operator, $\bar{\Gamma}$ and $\bar{\gamma}$ are the irreducible representation to which the lattice vibrations belong and the index of the row of $\bar{\Gamma}$ respectively.

If $D_{\bar{\gamma}\bar{\gamma}}^{(\bar{\Gamma})}(G)$ is the symmetry operation matrix representation, $g(\bar{\Gamma})$ the dimension of $\bar{\Gamma}$ and g the order of the group G , then the symmetrized displacement $\vec{Q}_{\bar{\Gamma}\bar{\gamma}}$ can be written as [23].

$$\vec{Q}_{\bar{\Gamma}\bar{\gamma}} = \frac{g(\bar{\Gamma})}{g} \sum_{\hat{G}} D_{\bar{\gamma}\bar{\gamma}}^{(\bar{\Gamma})}(\hat{G}) \hat{G} \Delta \vec{R}_\alpha \dots \dots \dots (7.6)$$

$\vec{Q}_{\bar{\Gamma}\bar{\gamma}}$ are transformed in the same manner as the normal coordinates. The summation is carried over all the symmetry operators \hat{G} . Performing the reverse transformation in eq.(7.6) and using eq.(7.3), \hat{H}_{eL} can be expressed as

$$\hat{H}_{el}(\vec{r}, \vec{q}) = \sum_{\vec{F}\vec{f}} \hat{V}_{\vec{F}\vec{f}}(\vec{r}) \vec{Q}_{\vec{F}\vec{f}} \dots \dots \dots (7.7)$$

where

$$\hat{V}_{\vec{F}\vec{f}} = \sum_{\alpha, i} \frac{\partial \hat{W}}{\partial R_{\alpha i}} \cdot \frac{\partial \vec{Q}_{\vec{F}\vec{f}}}{\partial R_{\alpha i}} \dots \dots \dots (7.8)$$

(i = x, y, z)

are the electronic irreducible tensor operators of the type \vec{F} and they transform like the corresponding symmetrized coordinates $\vec{Q}_{\vec{F}\vec{f}}$ under the symmetry operations of the point group [24] and

$$\vec{Q}_{\vec{F}\vec{f}} = \sum_{\vec{x}\nu} \left(\frac{\hbar}{M\omega_{\vec{x}\nu}} \right)^{1/2} \vec{A}_{\vec{x}\nu} q_{\vec{x}\nu} \dots \dots \dots (7.9)$$

where

ν is the branch of phonon spectra

\vec{x} is the phonon wave-vector.

M is the mass of the crystal lattice

$\omega_{\vec{x}\nu}$ is the phonon frequency

$q_{\vec{x}\nu}$ is the dimensionless normal coordinate of the lattice vibration.

$\vec{A}_{\vec{x}\nu}$ are the Van-Vleck coefficients given by the

expression

$$\vec{A}_{\vec{x}\nu} = \frac{g(\vec{F})}{g} \sum_{\hat{G}} D_{\vec{F}\vec{f}}^{(\vec{F})}(\hat{G}) \hat{G} \vec{e}_{\vec{x}\nu} e^{-i\vec{x}\vec{R}_{n_0}} \dots \dots \dots (7.10)$$

The cartesian displacements $\Delta \vec{R}$ are related to the normal coordinate $q_{\vec{x}\nu}$ of the lattice vibration through the

expression

$$\Delta \vec{R}_\alpha = \sum_{\vec{x}\nu} \left(\frac{\hbar}{M\omega_{\vec{x}\nu}} \right)^{1/2} \vec{e}_{\vec{x}\nu} q_{\vec{x}\nu} e^{-i\vec{x}\cdot\vec{R}} \dots\dots\dots (7.11)$$

where $\vec{e}_{\vec{x}\nu}$ is a unit vector in the direction of phonon polarization.

The Van-Vleck coefficients $\vec{a}_{\vec{x}\nu}$ appearing in eq. (7.9) satisfy the orthogonality relations,

$$\sum_{\vec{r}\vec{r}'} \vec{a}_{\vec{x}\nu}(\vec{r}\vec{r}) \vec{a}_{\vec{x}\nu'}(\vec{r}\vec{r}') = \delta_{\nu\nu'} \dots\dots\dots (7.12)$$

and

$$\sum_{\Omega\vec{x}} \vec{a}_{\vec{x}\nu}(\vec{r}\vec{r}) \vec{a}_{\vec{x}\nu'}(\vec{r}\vec{r}') = b_{\vec{x}\nu}(\vec{r}) \delta_{\vec{r}\vec{r}'} \delta_{\nu\nu'} \dots\dots\dots (7.13)$$

where $\sum_{\Omega\vec{x}}$ implies the integration along the direction of wave vector \vec{x} and averaging over the direction of the polarization vector $\vec{e}_{\vec{x}\nu}$ for a fixed direction of \vec{x} .

In the language of second quantization, the electron-phonon Hamiltonian operator \hat{H}_{eL} can be quantized by introducing the creation and annihilation operators $\hat{C}_{\vec{x}\nu}^+$ and $\hat{C}_{\vec{x}\nu}^-$ such that

$$q_{\vec{x}\nu} = \frac{1}{\sqrt{2}} (\hat{C}_{\vec{x}\nu} + \hat{C}_{\vec{x}\nu}^+) \dots\dots\dots (7.14)$$

and the quantized Hamiltonian (\hat{H}_{eL}) operator becomes

$$\hat{H}_{el} = \frac{1}{\sqrt{2}} \sum_{\vec{x}\nu} \left(\hat{V}_{\vec{x}\nu}^{*(F)} \hat{C}_{\vec{x}\nu} + \hat{V}_{\vec{x}\nu}^{(F)} \hat{C}_{\vec{x}\nu}^{\dagger} \right) \dots\dots (7.15)$$

with

$$\hat{V}_{\vec{x}\nu} = \sum_{\vec{r}\bar{r}} \hat{V}_{\vec{r}\bar{r}}^{(F)} \left(\frac{\hbar}{M\omega_{\vec{x}\nu}} \right)^{1/2} \vec{a}_{\vec{x}\nu} \dots\dots\dots (7.16)$$

This equation enables us to split the Hamiltonian eq.(7.15) into parts corresponding to irreducible representation of the lattice vibration.

8: Investigation of higher order elementary moments,
second and third moments.

If we restrict ourselves to the linear electron-phonon interaction, we find that the phonon contribution to the first moment vanishes i.e. $G_1=0$ and $G_0=1$ [25]. Applying the differentiation rule for the Heisenberg operators one can compute the k^{th} order derivatives in eq. (6.13) by successive differentiation of the evolution operator given in eq. (5.11). Using eq. (6.13) one obtains the second moment as

$$\hat{G}_2 = (i)^2 \left\langle \frac{d^2 \hat{U}(t)}{dt^2} \Big|_{t=0} \right\rangle_L \dots\dots\dots (8.1)$$

Differentiating eq. (5.11) one obtains

$$i\hbar \ddot{u}(t) = \hat{H}_{eL}(t) \dot{u}(t) + \dot{\hat{H}}_{eL}(t) u(t) \dots\dots\dots (8.2)$$

Using eq. (5.11) for $\dot{u}(t)$ one gets

$$i\hbar \ddot{u}(t) = \hat{H}_{eL}(t) \frac{1}{i\hbar} \hat{H}_{eL}(t) u(t) + \frac{1}{i\hbar} [\hat{H}_0, \hat{H}_{eL}] \dot{u}(t) \dots (8.3)$$

which on rearranging gives,

$$-\left\langle \frac{d^2}{dt^2} u(t) \Big|_{t=0} \right\rangle_L = -\frac{1}{\hbar^2} \left[\left\langle \hat{H}_{eL}^2 \dot{u}(t) \Big|_{t=0} \right\rangle_L + \left\langle [\hat{H}_0, \hat{H}_{eL}] \dot{u}(t) \Big|_{t=0} \right\rangle \right] \dots\dots\dots (8.4)$$

\hat{H}_0 is the zeroth-order Hamiltonian defined by

$$\hat{H}_0 = \hat{H}_e - \hbar \hat{W} \dots\dots\dots (8.5)$$

Since the commutator $[\hat{H}_0, \hat{H}_{eL}]$ is linear with respect to the phonon and therefore vanishes when phonon (L) average is taken, i.e. $\langle [\hat{H}_0, \hat{H}_{eL}] \rangle = 0$, eq. (8.4) becomes

$$-\left\langle \frac{d^2}{dt^2} u(t) \Big|_{t=0} \right\rangle_L = -\frac{1}{\hbar^2} \left\langle \hat{H}_{eL}^2 \right\rangle \dots\dots\dots (8.6)$$

Using the quantized Hamiltonian operator \hat{H}_{eL} , eq. (7.15), we finally get the expression for the second moment as

$$\hat{\sigma}_2 = \frac{1}{\hbar^2} \left\langle \hat{H}_{eL}^2 \right\rangle_L = \frac{1}{\hbar^2} \sum_{\vec{x}} \hat{v}_{\vec{x}}^* \hat{v}_{\vec{x}} \text{Coth} \frac{\beta \hbar \omega_{\vec{x}}}{2} \dots (8.7)$$

where

$$\beta_{\vec{\alpha}} = \frac{\hbar \omega}{k_B T}$$

Equation (8.7) shows that the second moment is perturbation independent.

Using eq. (7.16) and the orthogonality relation for Van-Vleck coefficients $\vec{a}_{\alpha\nu}$ eq. (7.13), the expression for the second moment becomes

$$\hat{Q}_2 = \frac{1}{2\hbar M} \sum_{\alpha\nu} \sum_{\vec{r}\vec{r}'} \frac{b_{\alpha\nu}(\vec{r})}{\omega_{\alpha\nu}} \coth \frac{\beta_{\vec{\alpha}}}{2} \hat{V}_{\vec{r}\vec{r}'}^+ \hat{V}_{\vec{r}\vec{r}'} \dots (8.8)$$

or

$$\hat{Q}_2 = \sum_{\vec{r}} Q_2(\vec{r}) \dots (8.9)$$

i.e. the total second moment is the sum of the contributions of each irreducible representation of lattice vibrations. In the same way the expression for third moment takes the form

$$\hat{Q}_3 = (-i)^3 \left\langle \frac{d^3 \hat{u}(t)}{dt^3} \Big|_{t=0} \right\rangle_L \dots (8.10)$$

The third derivative of eq. (5.11) yields

$$\ddot{\ddot{u}} = \frac{i}{\hbar^3} \left[\{ \hat{H}_b, [\hat{H}_b, \hat{H}_{el}] \} - 2 [\hat{H}_b, \hat{H}_{el}] \hat{H}_{el} - \hat{H}_{el} [\hat{H}_b, \hat{H}_{el}] + \hat{H}_{el}^3 \right] u(t) \dots (8.11)$$

Applying the well known commutation properties of the phonon operators, i.e.,

$$[\hat{C}_{\vec{x}}, \hat{C}_{\vec{x}}] = [\hat{C}_{\vec{x}}^+, \hat{C}_{\vec{x}}^+] = 0$$

$$[\hat{C}_{\vec{x}}, \hat{C}_{\vec{x}'}^+] = \delta_{\vec{x}\vec{x}'} \quad \dots (8.12)$$

and making use of the substitution

$$\hat{H}_0 = \hat{H}_L + \hbar\Omega_0 \hat{I} + \hbar\hat{W} \quad \dots (8.13)$$

the third moment is obtained with two parts as follows

$$\hat{O}_3^{(1)} = \frac{1}{\hbar^2} \sum_{\vec{x}} \omega_{\vec{x}} \hat{V}_{\vec{x}}^+ \hat{V}_{\vec{x}} = \frac{1}{2\hbar M} \sum_{\vec{x}} \sum_F b_{\vec{x}\nu(F)} \hat{V}_{F\bar{F}}^+ \hat{V}_{F\bar{F}} \quad \dots (8.14)$$

and

$$\begin{aligned} \hat{O}_3^{(2)} &= \frac{1}{\hbar^2} \sum_{\vec{x}} \text{Coth} \frac{\beta \hbar \omega_{\vec{x}}}{2} [\hat{V}_{\vec{x}}, \hat{W}] \hat{V}_{\vec{x}} \\ &= \frac{1}{2\hbar M} \sum_{\vec{x}\nu} \sum_{F\bar{F}} \frac{b_{\vec{x}\nu(F)}}{\omega_{\vec{x}\nu}} \text{Coth} \frac{\beta \hbar \omega_{\vec{x}\nu}}{2} [\hat{V}_{F\bar{F}}^+, \hat{W}] \hat{V}_{F\bar{F}} \quad \dots (8.15) \end{aligned}$$

so that

$$\hat{O}_3 = \hat{O}_3^{(1)} + \hat{O}_3^{(2)} \quad \dots (8.16)$$

$\hat{O}_3^{(1)}$ is the perturbation independent while $\hat{O}_3^{(2)}$ is linearly dependent on perturbation \hat{W} . The third moment is known to determine the asymmetry of the band shape. As can be seen, eq. (8.14), the perturbation independent part of the

third moment is temperature independent but the dependence on temperature comes in when the higher order EPI operator \hat{H}_{el} is taken into consideration. Finally the Jahn-Teller stabilization energy (ΔE^{J-T}) is given by the expression

$$\Delta E^{J-T} = \frac{1}{2M\hbar} \sum_{\vec{\alpha}} \sum_{\vec{r}\vec{\sigma}} \frac{b_{\vec{\alpha}\nu}(\vec{r})}{\omega_{\vec{\alpha}}^2} \hat{V}_{\vec{r}\vec{\sigma}}^+ \hat{V}_{\vec{r}\vec{\sigma}} \dots\dots (8.17)$$

and it will be discussed in detail in Chapter 3.

CHAPTER III

MOMENTS OF A \rightarrow T ABSORPTION BAND OF Co^{2+} IN CdF_2 AND CaF_2

As was stated earlier, the absorption band of impurity crystals consist of broad band, an indication of a strong electron-phonon interaction. The absorption band shape associated with transition from a singlet to an orbital triplet state was investigated intensively on F-centres in halides [26], F-centres in CaO [27, 28] and especially on the transitions ${}^1A_{1g} \rightarrow {}^1T_{1u}$ and ${}^1A_{1g} \rightarrow {}^3T_{1u}$ bands, i.e. A and C bands of heavy metal ions in alkali halides. This latter problem was theoretically treated in semiclassical approximation by Toyozawa and Inoue [8] and by Cho [9]. Their calculation of the absorption line based on the Frank-Condon approximation showed that strong linear interaction of an electronic triplet state with a triply degenerate T_2 -mode results in a symmetrical triple band. In this chapter the calculations for the second and third moments and Jahn-Teller stabilization energy (ΔE^{J-T}) will be done for both $\text{CdF}_2:\text{Co}^{2+}$ and $\text{CaF}_2:\text{Co}^{2+}$ systems. The triple absorption bands in this systems (see figs. 3 and 4) indicated a strong electron-phonon interaction, i.e, the main contribution is due to Jahn-Teller lattice vibrations.

9. Electron wavefunction of Co^{2+} in CdF_2 and CaF_2 .

The two systems (CdF_2 and CaF_2) are closely related, both having the same structure, the same anion and nearly the same crystal lattice constant (5.388 Å for CdF_2 and 5.463 Å for CaF_2). The structure of CdF_2 and CaF_2 can be viewed as a cubic close-packing cations with F^- ions occupying all the tetrahedral

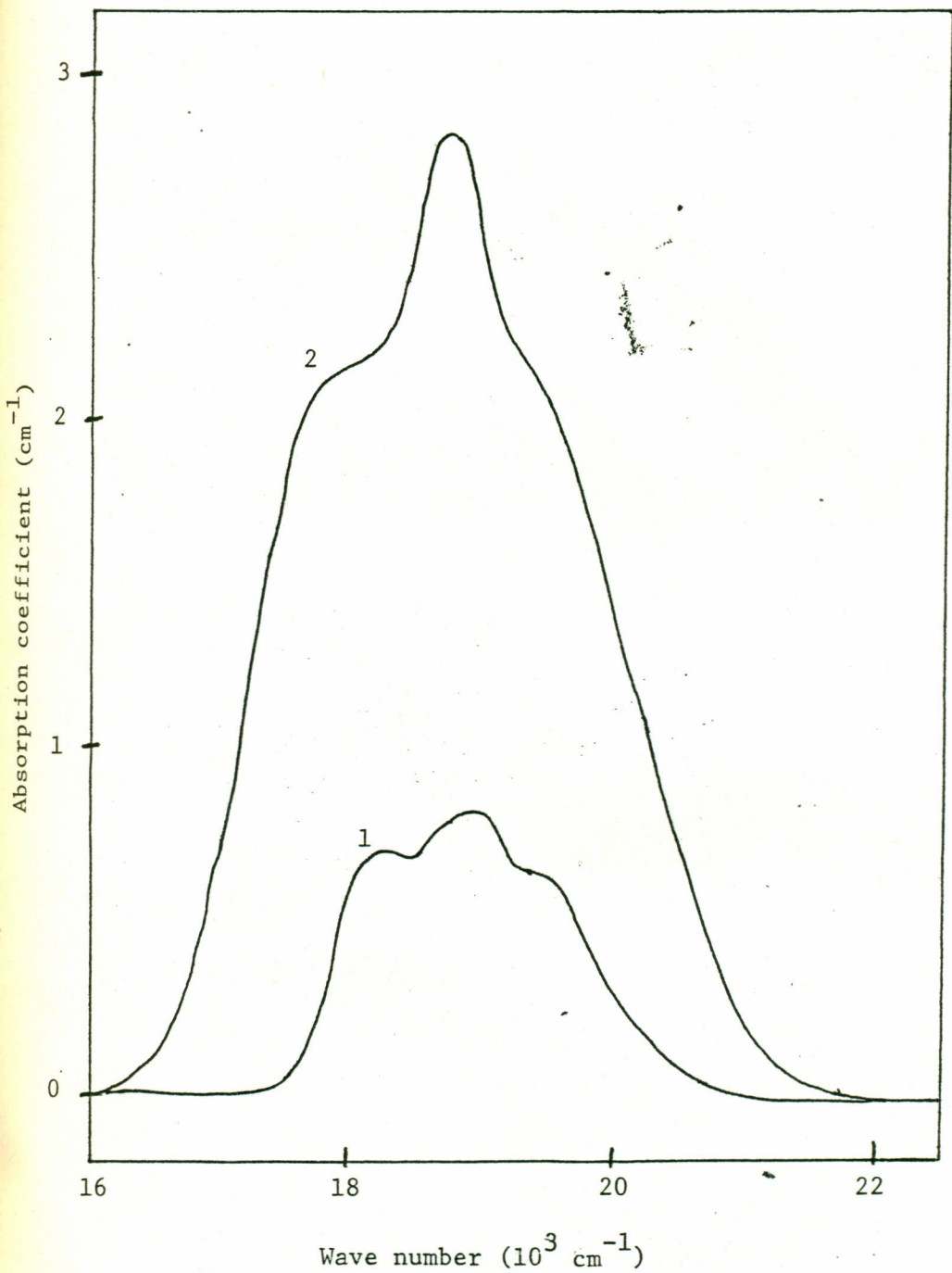


Fig. 3. The absorption spectra of a $\text{CdF}_2:\text{Co}^{2+}$ crystal at (1) 21K (2) 300K in the region of the ${}^4\text{A}_{2g} \longrightarrow {}^4\text{T}_{1g}(\text{P})$ transition [31].

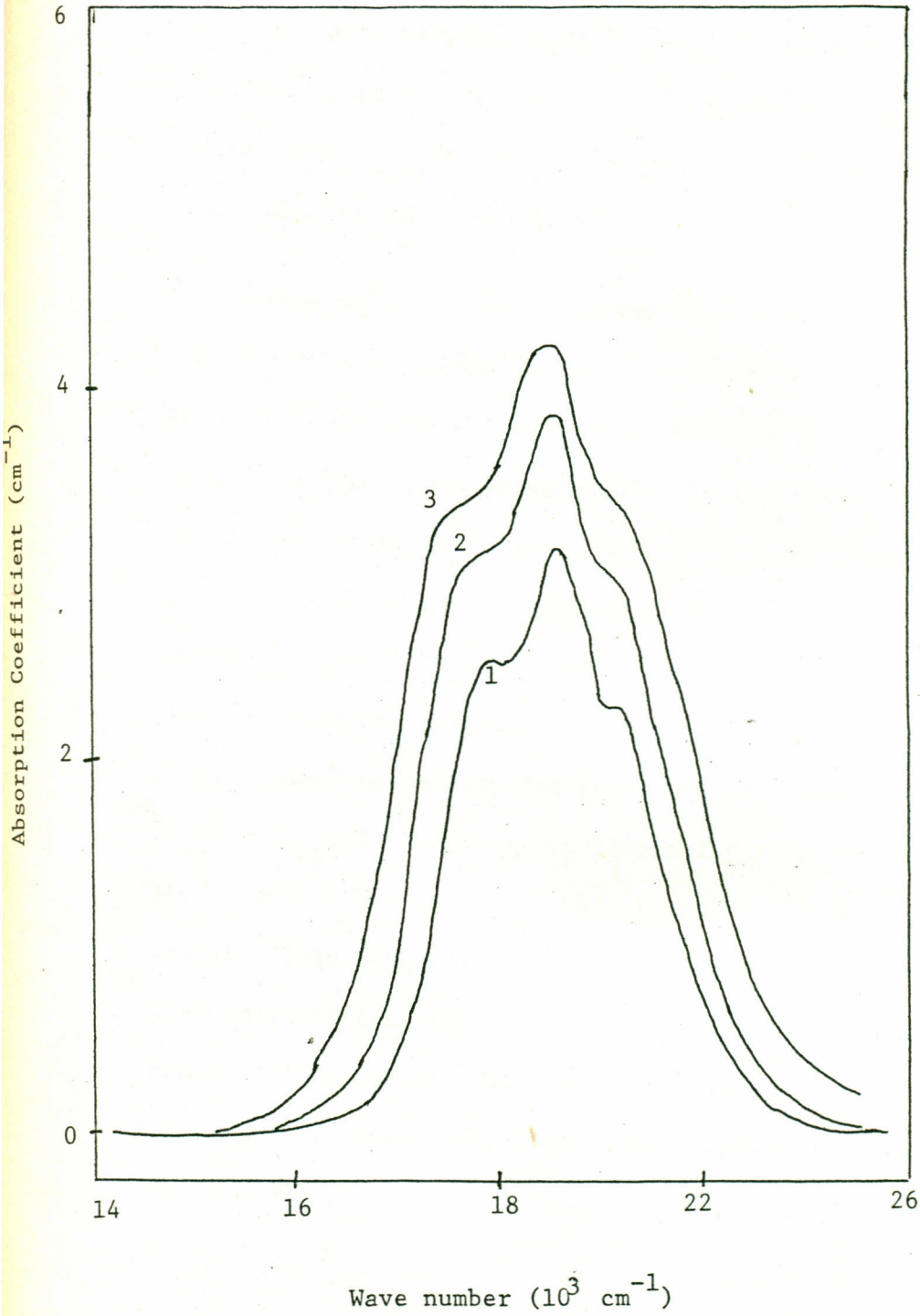


Fig. 4. The absorption spectra of a $\text{CaF}_2:\text{Co}^{2+}$ crystal at (1) 21K (2) 125K (3) 300K. in the region of the ${}^4\text{A}_{2g} \rightarrow {}^4\text{T}_{1g}(\text{P})$ transition. [32].

holes. In this structural framework, Cd^{2+} and Ca^{2+} ions are located at the centre of the cube of F^- anions. Each cation is therefore surrounded by eight F^- ions at the corners of the cube forming an MX_8 system of O_h symmetry (see fig. 5). In both systems the impurity ion Co^{2+} substitutes the Cd^{2+} and Ca^{2+} ions in the lattice sites randomly.

A free Co^{2+} ion has seven electrons (three holes) in its outermost shell ($3d^7$). Therefore the wave function for $3d^3$ will be derived which is equivalent to $3d^7$ configuration. In these systems, the intermediate crystal field scheme is applicable. That is, where $V_{ee} > V_c > V_{so}$, such that the 4F state of the free ion is split into 4A_2 , 4T_2 , 4T_1 and 4P state remains unsplit. V_{ee} , V_c and V_{so} are electron-electron, crystal field and spin-orbital interactions respectively. In these systems the absorption spectrum for $^4A_2 \rightarrow ^4T_{1g}(P)$ and $^4A_{2g} \rightarrow ^4T_{1g}(F)$ have been experimentally observed [31, 32]. The wavefunctions for $^4A_{2g}$ and 4T_1 are constructed in strong crystal field approximation with the help of single d-electron wavefunctions (t_{2g} and e_g wavefunctions), taking into consideration the intermixing of the states by Coulomb interaction. The single d-electron wavefunctions are as follows [29].

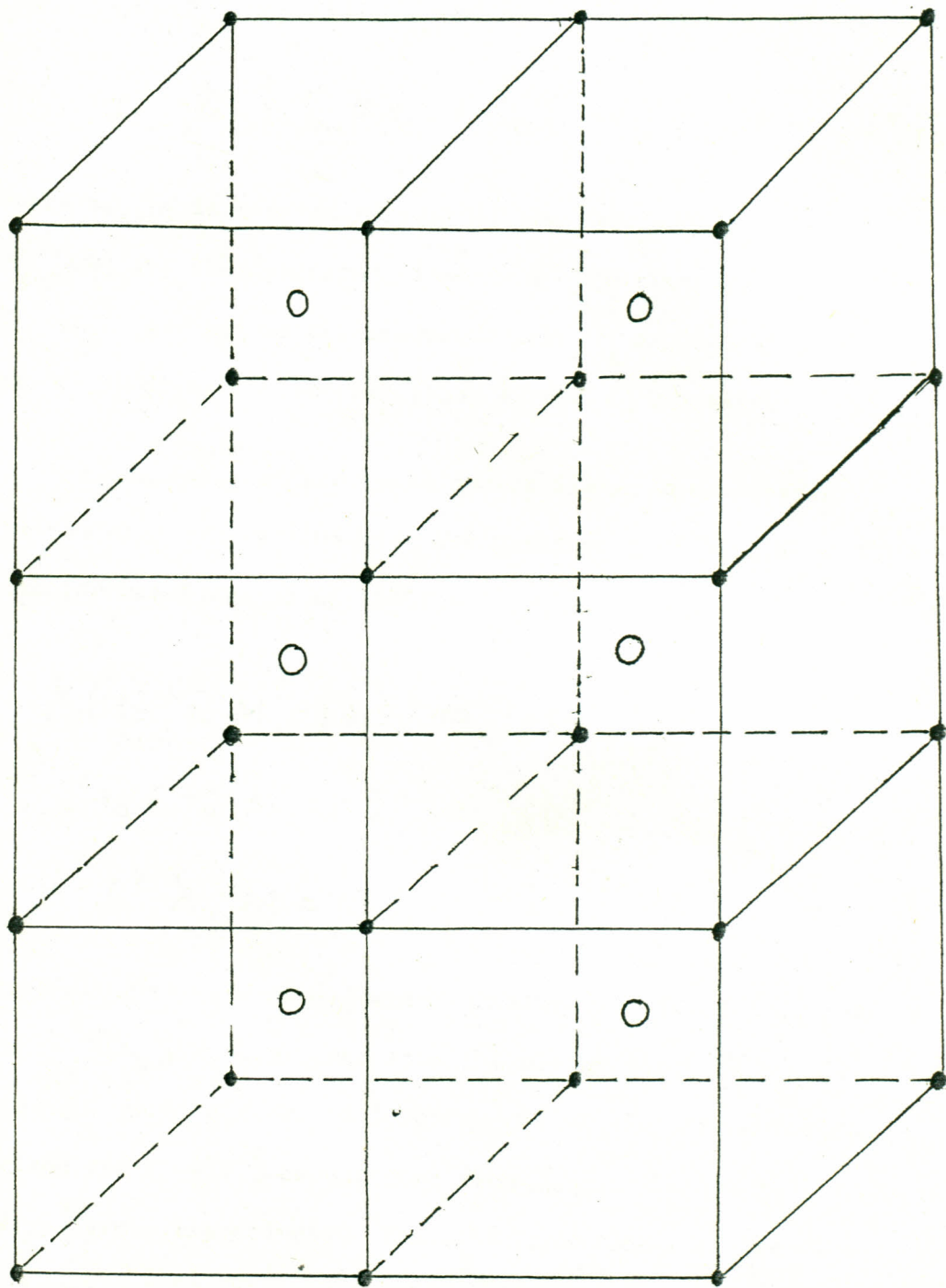
$$\xi = \frac{1}{\sqrt{2}} (Y_{2,1}(\theta, \varphi) + Y_{2,-1}(\theta, \varphi)) R_{3d}(r) \quad \dots (9.1a)$$

$$\dots (9.1b)$$

$$\eta = \frac{1}{\sqrt{2}} (Y_{2,-1}(\theta, \varphi) - Y_{2,1}(\theta, \varphi)) R_{3d}(r)$$

$$\dots (9.1c)$$

$$\zeta = \frac{1}{\sqrt{2}} (Y_{2,-2}(\theta, \varphi) + Y_{2,2}(\theta, \varphi)) R_{3d}(r)$$



● Fluoride ion. ○ Metal (impurity) ion

Fig. 5. The fluoride structure (MX_8 system) showing each metal ion (impurity ion) being surrounded by eight fluoride ions.

$$u = Y_{2,0}(\theta, \varphi) R_{3d}(r) \dots\dots\dots (9.2a)$$

$$v = \frac{1}{\sqrt{2}} (Y_{2,2}(\theta, \varphi) + Y_{2,-2}(\theta, \varphi)) R_{3d}(r) \dots\dots (9.2b)$$

where $R_{3d}(r)$ is the radial part of the wavefunction and $Y_{lm}(\theta, \varphi)$ are the spherical harmonics. The bases given by eq. (9.1) are the wavefunctions of the t_{2g} orbital while eq. (9.2) gives the wavefunctions of the e_g orbital.

Using the standard technique of Slater determinants, the two-electron wavefunction are obtained from single-electron wavefunction as follows

$$\Psi(t_2^2 \ ^3T_1, M = 1\alpha) = |\eta \zeta| \dots\dots\dots (9.3)$$

$$\Psi(t_2 e^2 \ ^3T_1, M = 1\alpha) = |\zeta \nu| \dots\dots\dots (9.4)$$

$$\Psi(e^2 \ ^3A_2, M = 1\alpha) = |u \nu| \dots\dots\dots (9.5)$$

Eq. (9.3) gives the two-electron wavefunction for the ground state $|^4A_2\rangle$ as determined from the energy term $S_0 T_0 = ^3T_1$ while eq. (9.4) and eq. (9.5) gives the wavefunctions for the excited state $|^4T_1\rangle$ constructed from $S_0 T_0 = ^3T_1$ and $S_0 T_0 = ^3A_2$ energy terms respectively. The other components of the wavefunctions can be obtained by the appropriate cyclic permutations of the bases ξ, η, ζ, u and ν .

Further, the three-electron wavefunctions for the states $^4A_2, ^4T_2 (t_2^2 e)$ and $^4T_1 (t_2 e^2)$ are derived by way of adding a system of one t_2' electron to a two t_2^2 electron system. This

is achieved with the help of the function [29].

$$\Psi'(t_2^2(s_0 r_0) t_2' s r) = \sum_{\substack{M_0, m_3 \\ \gamma_0, \gamma_3}} \Psi(t_2^2 s_0 r_0 M_0 \gamma_0) \phi(t_2' m_3 \gamma_3) \times \\ \langle s_0 M_0 \frac{1}{2} m_3 | SM \rangle \langle \Gamma_0 \gamma_0 T_2 \gamma_3 | \Gamma \gamma \rangle \dots (9.6)$$

where $\Psi(t_2^2 s_0 r_0 M_0 \gamma_0)$ is the wavefunction of t_2^2 involving electrons 1 and 2 and $\phi(t_2' m_3 \gamma_3)$ the spin-orbital of the added electron i.e electron 3. Here, t_2' orbital is taken to mean that it has the same symmetry as that of t_2 but different from t_2 orbital. This function i.e eq. (9.6) is base γ of irreducible representation Γ of O_h group. Though this function is antisymmetric with respect to electrons 1 and 2, it is not with respect to electron exchange 1, 3 and 2, 3. The function is made antisymmetric with respect to all the electrons but must remain an eigenfunction of \bar{S}^2 and S_z , where \bar{S} is the resultant spin-angular momentum.

Antisymmetrizing the function and using the appropriate properties of determinants one obtains.

$$\Psi(t_2^2(s_0 r_0) t_2' s r M \gamma) = \sum_{K_1, K_2, K_3} C_{K_1, K_2, K_3} \begin{vmatrix} \phi_{K_1} & \phi_{K_2} & \phi_{K_3} \end{vmatrix} \dots (9.7)$$

where K_i represents set of quantum numbers $(t_2 m_i \gamma_i)$ for $i = 1, 2$ and K_3 represents $(t_2' m_3 \gamma_3)$. C_i are numerical constants to be determined from eq. (9.6). Using eq. (9.6) and eq. (9.7) the three-electron normalized wavefunctions for the states 4A_2 , ${}^4T_1(t_2^2 e)$ and ${}^4T_1(t_2 e^2)$ are found to be

$$\Psi(t_2^3 ({}^3\bar{1}_1) {}^4A_2, M=3/2, \chi) = -|\eta \xi \zeta| \dots (9.8a)$$

$$\Psi(t_2^2 ({}^3\bar{1}_1) e {}^4\bar{1}_1, M=3/2, \chi) = |\eta \xi u| \dots (9.8b)$$

$$\Psi(e^2 ({}^3A_2) t_2' {}^4\bar{1}_1, M=3/2, \chi) = -|\mu v \xi| \dots (9.8c)$$

The two electronic states arising from $t_2^2 e$ and $t_2 e^2$ whose wavefunctions are given by eq. (9.8b) and eq. (9.8c) are admixed due to the Coulomb interaction (electron configuration mixing) resulting in shifts of their energies. The term energies of two 4T_1 states are calculated by solving the secular equation

$$\begin{vmatrix} t_2^2 & 2\langle g|f|g\rangle + J(\xi\eta) - K(\xi\eta) - E & 2\langle \xi\eta|g\nu\rangle \\ t_2 e & 2\langle \xi\eta|g\nu\rangle & \langle g|f|g\rangle + \langle \nu|f|\nu\rangle + J(g\nu) - K(g\nu) - E \end{vmatrix} = 0 \dots (9.9)$$

where $J(\chi\chi')$ and $K(\chi\chi')$ are the Coulomb integral and exchange integral respectively and

$$\langle \nu|f|\nu\rangle - \langle g|f|g\rangle = 10Dq \dots (9.10)$$

The two states are termed as ${}^4T_1(P)$ and ${}^4T_1(F)$ states.

Expressing the integrals in terms of crystal field parameter Dq and Racah parameter B , the wavefunctions for the two states ${}^4T_1(P)$ and ${}^4T_1(F)$ can be written as

$$|{}^4\bar{1}_1(P)\rangle = \cos\theta \Psi(t_2^2 e) - \sin\theta \Psi(t_2 e^2) \dots (9.11a)$$

$$|{}^4\bar{1}_1(F)\rangle = \sin\theta \Psi(t_2^2 e) + \cos\theta \Psi(t_2 e^2) \dots (9.11b)$$

where

$$\tan 2\theta = \frac{12B}{10Dq - 9B}$$

The values of Dq and Racah parameter B are shown in the table below.

TABLE 1. The Crystal Field Parameters and the Racah Parameters

	CdF ₂ :Co ²⁺ [31]	CaF ₂ :Co ²⁺ [33]
Dq (cm ⁻¹)	400	360
B (cm ⁻¹)	930	930

Finally, in the zeroth order approximation, the normalized wavefunctions for these states are obtained as follows

$$|{}^4T_1(P)\rangle_\alpha = \frac{1}{\sqrt{6}}[-|\eta\xi\mu| + \sqrt{3}|\eta\xi\nu|] + \frac{5}{9}|\mu\nu\xi| \quad \dots (9.12a)$$

$$|{}^4T_1(P)\rangle_\beta = -\frac{1}{\sqrt{6}}[|\xi\xi\mu| + |\xi\xi\nu|] + \frac{5}{9}|\mu\nu\eta| \quad \dots (9.12b)$$

$$|{}^4T_1(P)\rangle_\gamma = \sqrt{\frac{2}{3}}|\eta\xi\mu| + \frac{5}{9}|\mu\nu\xi| \quad \dots (9.12c)$$

$$|{}^4T_1(F)\rangle_\alpha = -\frac{5}{18}[-|\eta\xi\mu| + \sqrt{3}|\eta\xi\nu|] - \sqrt{\frac{2}{3}}|\mu\nu\xi| \quad \dots (9.12d)$$

$$|{}^4T_1(F)\rangle_\beta = \frac{5}{18}[|\xi\xi\mu| + |\xi\xi\nu|] - \sqrt{\frac{2}{3}}|\mu\nu\eta| \quad \dots (9.12e)$$

$$|{}^4T_1(F)\rangle_\gamma = -\frac{5}{9}|\eta\xi\mu| - \sqrt{\frac{2}{3}}|\mu\nu\xi| \quad \dots (9.12f)$$

Since the Dq values for both $\text{CdF}_2:\text{Co}^{2+}$ and $\text{CaF}_2:\text{Co}^{2+}$ are close and the values of the Racah parameter B for the two systems are the same, the three-electron wavefunctions eq.(9.12) holds true to both systems.

10. The Electron-Phonon Interaction operator

As was pointed out earlier the electronic configuration of Co^{2+} is $3d^7$ and it is surrounded by eight ligands (MX_8). Considering only the first eight nearest neighbour ions of the impurity centre, the potential energy \hat{W}_c of the electrons of the central ion (Co^{2+}) in a system having O_h symmetry can be expressed as

$$\hat{W}_c = \sum_{k=1,2,3} \sum_{\alpha=1}^8 \frac{ee^*}{4\pi\epsilon_0 |\vec{R}_\alpha - \vec{r}_k|} \dots\dots\dots (10.1)$$

where e^* is the effective charge of the α^{th} lattice point and e is the charge of the electron of impurity centre. $\alpha = 1, 2, \dots, 8$ represents the eight point charges (nearest neighbours) and $k=1, 2, 3$ are the three electrons of the Co^{2+} ion. \vec{R}_α is the position vector of the α^{th} point charge and \vec{r}_k is the position vector of the electron. Taking W_c to be a small perturbation, it is expanded in Legendre polynomial as

$$W_c(\vec{r}, \vec{R}_\alpha) = \frac{ee^*}{4\pi\epsilon_0} \sum_{\alpha=1}^8 \sum_{l=0}^{\infty} \frac{Y_l^m}{Y_l^{l+1}} P_l(\cos \omega_\alpha) \dots\dots (10.2)$$

where ω_α is the angle between \vec{R} and \vec{r}_k and \vec{r}_k and \vec{R} are the lesser than and greater than \vec{R} respectively. Without loss of generality, \vec{r}_k and \vec{R} can be written as \vec{r} and \vec{R}_α respectively such that eq. (10.2) becomes,

$$W_c(\vec{r}, \vec{R}_\alpha) = \frac{ee^*}{4\pi\epsilon_0} \sum_{\alpha=1}^8 \sum_{l=0}^{\infty} \frac{r^l}{R_\alpha^{l+1}} P_l(\cos \omega_\alpha) \dots (10.3)$$

The addition theorem of spherical harmonics yields $P_l(\cos \omega_\alpha)$ as [29]

$$P_l(\cos \omega_\alpha) = \frac{4\pi}{2l+1} \sum_{m=-l}^l Y_{l,m}(\theta, \varphi) Y_{l,m}^*(\theta_\alpha, \varphi_\alpha), \dots (10.4)$$

where $Y_{l,m}(\theta, \varphi)$ and $Y_{l,m}^*(\theta_\alpha, \varphi_\alpha)$ are the spherical harmonics and their complex conjugate related through the expression

$$Y_{l,m}^*(\theta_\alpha, \varphi_\alpha) = (-1)^m Y_{l,-m}(\theta_\alpha, \varphi_\alpha) \dots (10.5)$$

and \vec{r}, θ, φ and $\vec{R}_\alpha, \theta_\alpha, \varphi_\alpha$ are the polar coordinates of \vec{r} and \vec{R} respectively. For the systems $\text{CdF}_2:\text{Co}^{2+}$ and $\text{CaF}_2:\text{Co}^{2+}$ which are body centred cubic, Fig. (5), the values of $(\theta_\alpha, \varphi_\alpha)$ for the eight nearest neighbours have been found to be as shown in table 2.

Substituting eq. (10.4) into eq. (10.3) the expression for \hat{W}_c becomes

$$\hat{W}_c(\vec{r}, \vec{R}_\alpha) = \frac{ee^*}{4\pi\epsilon_0} \sum_{\alpha=1}^8 \sum_{l=0}^{\infty} \sum_{m=-l}^l \left(\frac{4\pi}{2l+1} \right) \frac{r^l}{R_\alpha^{l+1}} Y_{l,m}(\theta, \varphi) Y_{l,m}^*(\theta_\alpha, \varphi_\alpha) \dots (10.6)$$

For d-state of the electron in O_h symmetry, the non-zero contribution in $\hat{W}_c(\vec{r}, \vec{R}_\alpha)$ is given by the terms with $l = 0, 2, 4$ such that eq. (10.6) becomes

TABLE 2. Values of $(\theta_\alpha, \varphi_\alpha)$ for the eight ligands of an MX_8 system.

Ligand	θ_α	φ_α
1	$\cos^{-1} (1/\sqrt{3})$	$\pi/4$
2	$\pi - \cos^{-1} (1/\sqrt{3})$	$3\pi/4$
3	$\pi - \cos^{-1} (1/\sqrt{3})$	$7\pi/4$
4	$\cos^{-1} (1/\sqrt{3})$	$5\pi/4$
5	$\cos^{-1} (1/\sqrt{3})$	$3\pi/4$
6	$\pi - \cos^{-1} (1/\sqrt{3})$	$\pi/4$
7	$\cos^{-1} (1/\sqrt{3})$	$7\pi/4$
8	$\pi - \cos^{-1} (1/\sqrt{3})$	$5\pi/4$

$$\begin{aligned} \hat{W}(\vec{r}, \vec{R}_\alpha) = 4\pi \left(\frac{ee^*}{4\pi\epsilon_0} \right) & \left[\sum_{\alpha=1}^8 \frac{1}{R_\alpha} Y_{00}(\theta, \varphi) Y_{00}^*(\theta_\alpha, \varphi_\alpha) \right. \\ & + \sum_{\alpha=1}^8 \sum_{m=-2}^2 \frac{Y^2}{5R_\alpha^3} Y_{2m}(\theta, \varphi) Y_{2m}^*(\theta_\alpha, \varphi_\alpha) \\ & \left. + \sum_{\alpha=1}^8 \sum_{m=-4}^4 \frac{Y^4}{9R_\alpha^5} Y_{4m}(\theta, \varphi) Y_{4m}^*(\theta_\alpha, \varphi_\alpha) \right] \dots (10.7a) \end{aligned}$$

The electron tensor operator \hat{V}_{ff} eq. (7.8) for an MX_8 system in cartesian coordinates is expressed as

$$\hat{V}_{\bar{r}\bar{s}} = \sum_{\alpha=1}^8 \left[\frac{\partial \hat{W}_c}{\partial R_{\alpha x}} \cdot \frac{\partial Q_{\bar{r}\bar{i}}}{\partial R_{\alpha x}} + \frac{\partial \hat{W}_c}{\partial R_{\alpha y}} \cdot \frac{\partial Q_{\bar{r}\bar{i}}}{\partial R_{\alpha y}} + \frac{\partial \hat{W}}{\partial R_{\alpha z}} \cdot \frac{\partial Q_{\bar{r}\bar{i}}}{\partial R_{\alpha z}} \right] \dots (10.7b)$$

Now, the differentiation of spherical harmonics which appear in eq. (10.7b) above is carried out with the help of the following equations [30].

$$\begin{aligned} \frac{\partial}{\partial R_{\alpha x}} \left[\frac{1}{R^{l+1}} Y_{l,m}^* (\theta_\alpha, \varphi_\alpha) \right] &= \frac{2l+1}{2R_\alpha^{l+2}} \left[\left\{ \frac{(l+m+2)(l-m+1)}{(2l+3)(2l+1)} \right\}^{1/2} Y_{l+1,m+1}^* (\theta_\alpha, \varphi_\alpha) \right. \\ &\quad \left. - \left\{ \frac{(l-m+2)(l-m+1)}{(2l+3)(2l+1)} \right\}^{1/2} Y_{l+1,m-1}^* (\theta_\alpha, \varphi_\alpha) \right] \dots (10.8a) \end{aligned}$$

$$\begin{aligned} \frac{\partial}{\partial R_{\alpha y}} \left[\frac{1}{R^{l+1}} Y_{l,m}^* (\theta_\alpha, \varphi_\alpha) \right] &= \frac{i(2l+1)}{2R_\alpha^{l+2}} \left[\left\{ \frac{(l+m+2)(l-m+1)}{(2l+3)(2l+1)} \right\}^{1/2} Y_{l+1,m+1}^* (\theta_\alpha, \varphi_\alpha) \right. \\ &\quad \left. + \left\{ \frac{(l-m+2)(l-m+1)}{(2l+3)(2l+1)} \right\}^{1/2} Y_{l+1,m-1}^* (\theta_\alpha, \varphi_\alpha) \right] \dots (10.8b) \end{aligned}$$

$$\frac{\partial}{\partial R_{\alpha z}} \left[\frac{1}{R^{l+1}} Y_{l,m}^* (\theta_\alpha, \varphi_\alpha) \right] = \frac{-(2l+1)}{R_\alpha^{l+2}} \left\{ \frac{(l+m+1)(l-m+1)}{(2l+3)(2l+1)} \right\}^{1/2} Y_{l+1,m}^* (\theta_\alpha, \varphi_\alpha) \dots (10.8c)$$

The symmetrized displacements are determined with the help of projection operator eq. (7.6), which gives the symmetrized displacements in trigonal coordinate system as follows

$$Q_{A_{1g}} = \frac{1}{\sqrt{2}} (Z_1 + Z_2 + Z_3 + Z_4 + Z_5 + Z_6 + Z_7 + Z_8) \dots \dots \dots (10.9a)$$

$$Q_{E_u} = \frac{1}{2\sqrt{2}} (X_1 - X_2 - X_3 + X_4 + X_5 - X_6 + X_7 - X_8) \dots \dots \dots (10.9b)$$

$$Q_{E_v} = \frac{1}{2\sqrt{2}} (Y_1 - Y_2 - Y_3 + Y_4 - Y_5 + Y_6 - Y_7 + Y_8) \dots \dots \dots (10.9c)$$

$$Q_{T_{2g}} = \frac{1}{\sqrt{2}} (Z_1 + Z_2 - Z_3 - Z_4 - Z_5 - Z_6 + Z_7 + Z_8) \dots \dots \dots (10.9d)$$

$$Q_{T_{2g}} = \frac{1}{2\sqrt{2}} (Z_1 - Z_2 + Z_3 - Z_4 + Z_5 - Z_6 - Z_7 + Z_8) \dots \dots \dots (10.9e)$$

$$Q_{T_{2g}} = \frac{1}{2\sqrt{2}} (Z_1 - Z_2 - Z_3 + Z_4 - Z_5 + Z_6 - Z_7 + Z_8) \dots \dots \dots (10.9f)$$

The local ligand trigonal coordinate system for MX_8 is shown in fig. (6). The active lattice vibration modes which are interacting with the electronic excited states ${}^4T_1(P)$ and ${}^4T_1(F)$ are represented by

$$[T_1^2] = A_{1g} + E_g + T_{2g}$$

where

- A_{1g} - totally symmetrical lattice vibration
- E_g - two-fold tetragonal lattice vibration
- T_{2g} - three-fold trigonal lattice vibration

The displacements of ligands for A_{1g} , E_g and T_{2g} modes of lattice vibrations are shown in figs. 7, 8 and 9.

Using the transformation eq. (10.10) below (see fig. 10),

$$X = \frac{1}{\sqrt{6}} (X + Y + 2Z) \dots \dots \dots (10.10a)$$

$$Y = \frac{1}{\sqrt{2}} (X - Y) \dots \dots \dots (10.10b)$$

$$Z = \frac{1}{\sqrt{3}} (X + Y + Z) \dots \dots \dots (10.10c)$$

the final expressions for the symmetrized displacements in

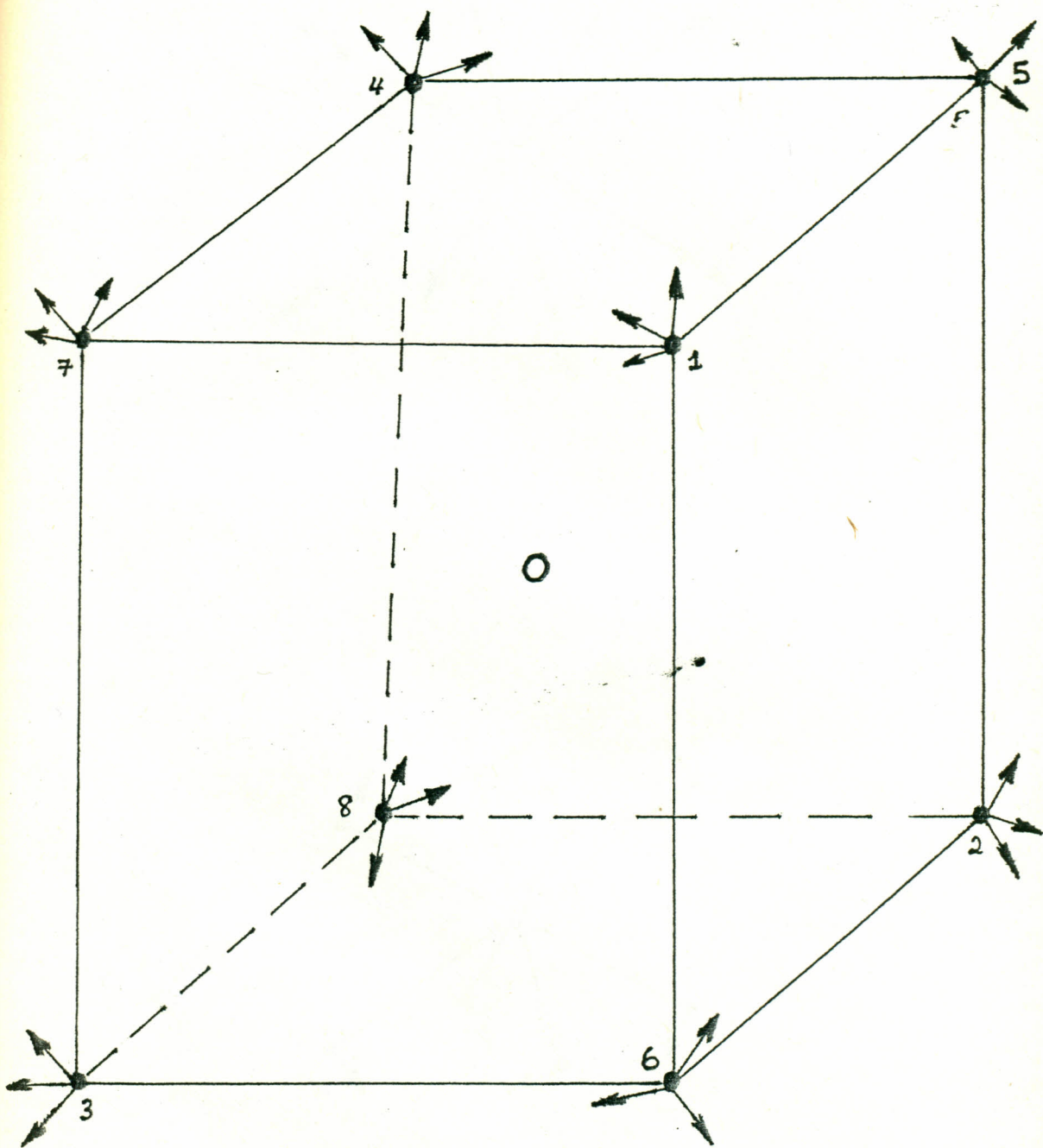
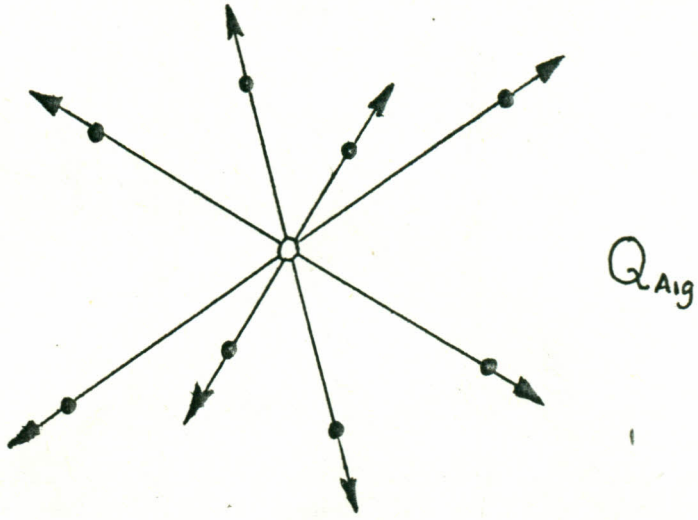
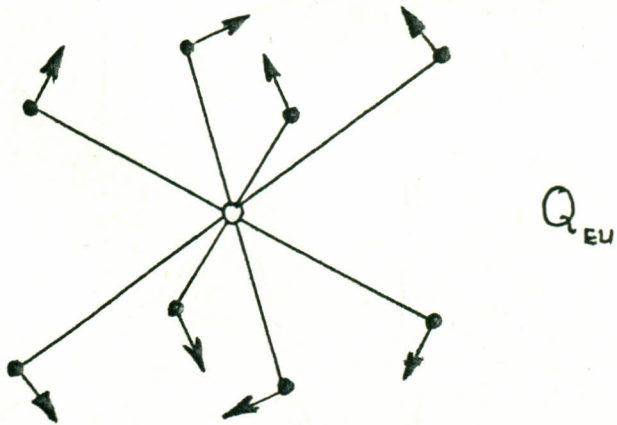


Fig. 6. Local ligand coordinate system for an MX_8 system.

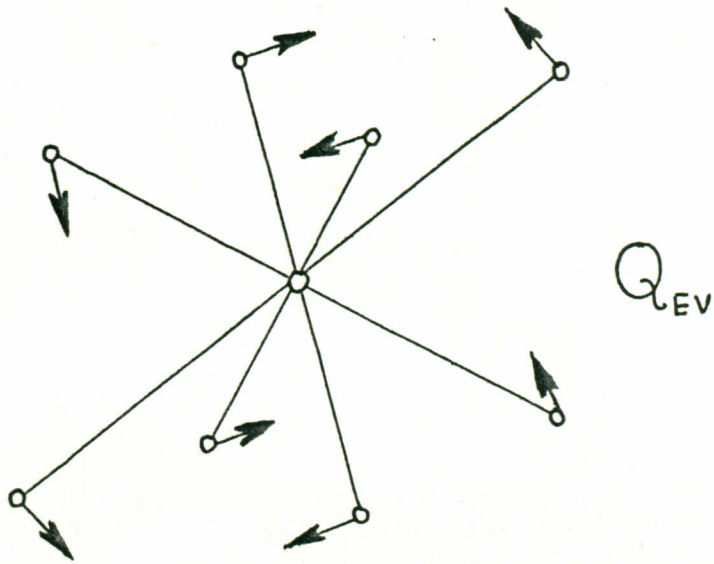


(a)

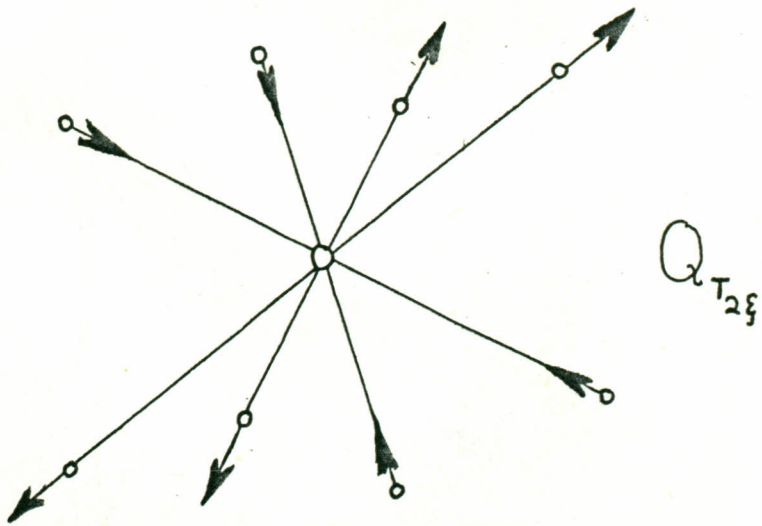


(b)

Fig. 7. Symmetrized displacements for (a) A_{1g} - mode and (b) E_g -mode of lattice vibration of MX_8 system.

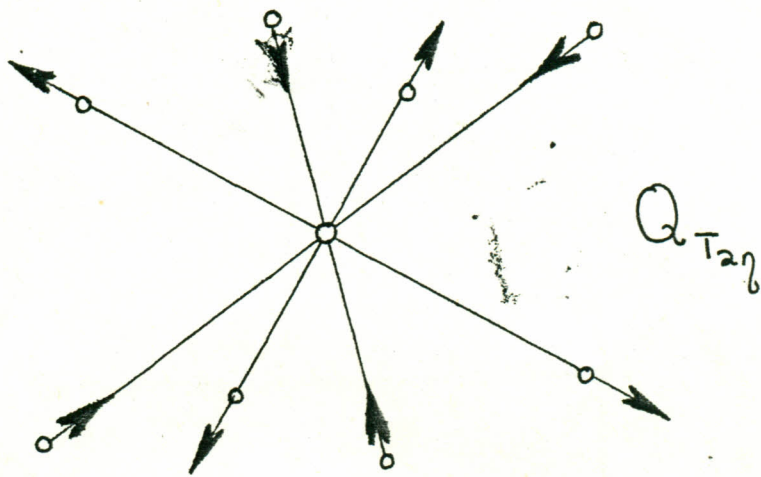


(a)

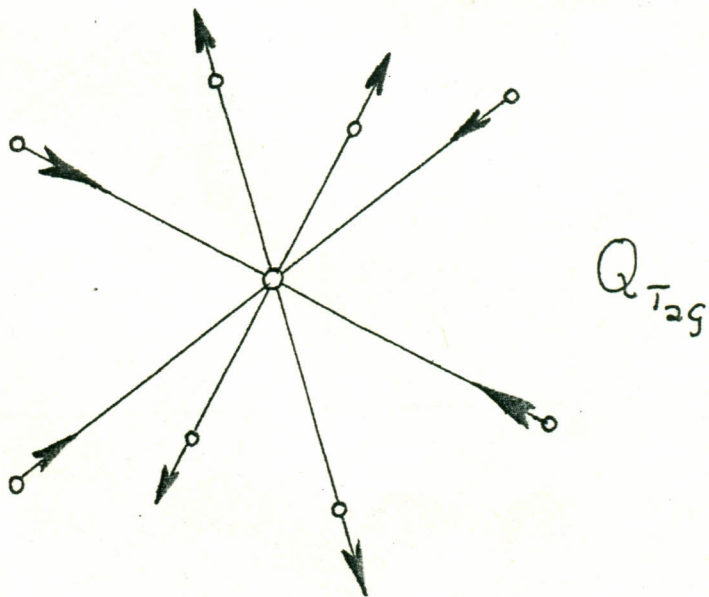


(b)

Fig. 8. Symmetrized displacements for (a) E_g -mode and (b) T_{2g} -mode of lattice vibration of MX_8 system.



(a)



(b)

Fig. 9. Symmetrized displacements for T_{2g} -mode of lattice vibration of MX_8 system.

tetragonal coordinate system becomes

$$Q_{A1g} = \frac{1}{2}\sqrt{6} \left[(X_1 - X_2 + X_3 - X_4 - X_5 + X_6 + X_7 - X_8) \right. \\ \left. + (Y_1 + Y_2 - Y_3 - Y_4 + Y_5 + Y_6 - Y_7 - Y_8) \right. \\ \left. + (Z_1 - Z_2 - Z_3 + Z_4 + Z_5 - Z_6 + Z_7 - Z_8) \right] \\ \dots (10.11a)$$

$$Q_{Eu} = \frac{1}{4}\sqrt{3} \left[(-X_1 + X_2 - X_3 + X_4 + X_5 - X_6 - X_7 + X_8) \right. \\ \left. + (-Y_1 - Y_2 + Y_3 + Y_4 - Y_5 - Y_6 + Y_7 + Y_8) \right. \\ \left. + 2(Z_1 - Z_2 - Z_3 + Z_4 + Z_5 - Z_6 + Z_7 - Z_8) \right] \\ \dots (10.11b)$$

$$Q_{Ev} = \frac{1}{4} \left[(X_1 - X_2 + X_3 - X_4 - X_5 + X_6 + X_7 - X_8) \right. \\ \left. + (-Y_1 - Y_2 + Y_3 + Y_4 - Y_5 - Y_6 + Y_7 + Y_8) \right] \\ \dots (10.11c)$$

$$Q_{T2g} = \frac{1}{2}\sqrt{6} \left[(X_1 - X_2 - X_3 + X_4 + X_5 - X_6 + X_7 - X_8) \right. \\ \left. + (Y_1 + Y_2 + Y_3 + Y_4 - Y_5 - Y_6 - Y_7 - Y_8) \right. \\ \left. + (Z_1 - Z_2 + Z_3 - Z_4 - Z_5 + Z_6 + Z_7 - Z_8) \right] \\ \dots (10.11d)$$

$$Q_{T2g} = \frac{1}{2}\sqrt{6} \left[(X_1 + X_2 + X_3 + X_4 - X_5 - X_6 - X_7 - X_8) \right. \\ \left. + (Y_1 - Y_2 - Y_3 + Y_4 + Y_5 - Y_6 + Y_7 - Y_8) \right. \\ \left. + (Z_1 + Z_2 - Z_3 - Z_4 + Z_5 + Z_6 - Z_7 - Z_8) \right] \\ \dots (10.11e)$$

$$Q_{T2g} = \frac{1}{2}\sqrt{6} \left[(X_1 + X_2 - X_3 - X_4 + X_5 + X_6 - X_7 - X_8) \right. \\ \left. + (Y_1 - Y_2 + Y_3 - Y_4 - Y_5 + Y_6 + Y_7 - Y_8) \right. \\ \left. + (Z_1 + Z_2 + Z_3 + Z_4 - Z_5 - Z_6 - Z_7 - Z_8) \right] \\ \dots (10.11f)$$

Using eqs. (10.7a), (10.7b), (10.8) and (10.11), and without showing the lengthy though elementary calculations, the expressions for $\hat{V}_{F\bar{F}}$ are obtained as follows

$$\hat{V}_{A_1} = -\frac{1}{3}\sqrt{\frac{5}{3}} \frac{Y_{00}(\theta, \varphi)}{R^2} + \frac{1}{27}\sqrt{\frac{5}{3}} \frac{Y^4}{R^6} Y_{4,0}(\theta, \varphi) + \frac{1}{18}\sqrt{\frac{35}{3}} \frac{Y^4}{R^6} (Y_{4,4}(\theta, \varphi) + Y_{4,-4}(\theta, \varphi)) \dots (10.12a)$$

$$\hat{V}_{E_u} = -\frac{2}{3}\sqrt{\frac{1}{3}} \frac{1}{R^2} Y_{0,0}(\theta, \varphi) + \frac{4}{3}\sqrt{\frac{1}{5}} \frac{Y^2}{R^4} Y_{2,0}(\theta, \varphi) + \frac{5}{27}\sqrt{\frac{1}{3}} \frac{Y^4}{R^6} Y_{4,0}(\theta, \varphi) + \frac{1}{9}\sqrt{\frac{35}{27}} \frac{Y^4}{R^6} (Y_{4,4}(\theta, \varphi) + Y_{4,-4}(\theta, \varphi)) \dots (10.12b)$$

$$\hat{V}_{E_g} = -\frac{4}{3}\sqrt{\frac{1}{3}} \frac{Y^2}{R^4} (Y_{2,2}(\theta, \varphi) - Y_{2,-2}(\theta, \varphi)) \dots (10.12c)$$

$$\hat{V}_{T_{2g}} = \frac{7}{3}\sqrt{\frac{1}{15}} \frac{Y^2}{R^4} (Y_{2,1}(\theta, \varphi) - Y_{2,-1}(\theta, \varphi)) + \frac{1}{27}\sqrt{\frac{35}{27}} \frac{Y^4}{R^6} (Y_{4,1}(\theta, \varphi) - Y_{4,-1}(\theta, \varphi)) + \frac{1}{9}\sqrt{\frac{35}{27}} \frac{Y^4}{R^6} (Y_{4,3}(\theta, \varphi) - Y_{4,-3}(\theta, \varphi)) \dots (10.12d)$$

$$\hat{V}_{T_{2g}} = -\frac{7i}{3}\sqrt{\frac{1}{15}} \frac{Y^2}{R^4} (Y_{2,1}(\theta, \varphi) + Y_{2,-1}(\theta, \varphi)) - \frac{i}{9}\sqrt{\frac{35}{81}} \frac{Y^4}{R^6} (Y_{4,3}(\theta, \varphi) + Y_{4,-3}(\theta, \varphi)) - \frac{i}{27}\sqrt{\frac{35}{27}} \frac{Y^4}{R^6} (Y_{4,1}(\theta, \varphi) + Y_{4,-1}(\theta, \varphi)) \dots (10.12e)$$

$$\hat{V}_{T_{2g}} = \frac{i}{6}\sqrt{\frac{5}{3}} \frac{Y^2}{R^4} (Y_{2,2}(\theta, \varphi) - Y_{2,-2}(\theta, \varphi)) \dots (10.12f)$$

Since $\hat{V}_{F\bar{F}}$ is one-electron operator, its matrix element between three-electron Slater determinant wavefunctions

$|\gamma_1 \gamma_2 \gamma_3\rangle$ can be expanded as follows [29]

$$\langle |\gamma_1 \gamma_2 \gamma_3\rangle | \hat{V}_{F\bar{F}} | |\gamma_1 \gamma_2 \gamma_3\rangle = \langle \gamma_1 | \hat{V}_{F\bar{F}} | \gamma_1 \rangle + \langle \gamma_2 | \hat{V}_{F\bar{F}} | \gamma_2 \rangle + \langle \gamma_3 | \hat{V}_{F\bar{F}} | \gamma_3 \rangle \dots (10.13)$$

where γ_i represents any of the bases η, ξ, ζ, μ and ν of irreducible representation Γ . Using the wavefunctions for 4A_2 , ${}^4T_1(P)$ and ${}^4T_1(F)$, eqs. (9.8a) and (9.12) and with the help of eq. (10.13) and the standard integration for three spherical harmonics [30],

$$\begin{aligned} \langle l_1, m_1 | Y_{l_1 m_1}^* | l_2, m_2 \rangle &= \int Y_{l_1 m_1} Y_{l_1 m_1}^* Y_{l_2 m_2} d\bar{\tau} \\ &= (-1)^{m_1} \left[\frac{(2l_1+1)(2l_2+1)(2l_2+1)}{4\pi} \right]^{1/2} \begin{pmatrix} l_1 & l & l_2 \\ -m_1 & m_1 & m_2 \end{pmatrix} \begin{pmatrix} l_1 & l & l_2 \\ 0 & 0 & 0 \end{pmatrix} \end{aligned} \quad \dots (10.14)$$

the expressions of the matrix elements of operator \hat{V}_{FF} are obtained as follows;

$$\langle {}^4A_2 | \hat{V}_{A_1} | {}^4A_2 \rangle = \left(\frac{1}{42\pi} \sqrt{\frac{5}{2}} - \frac{5\sqrt{3}}{36\pi} \right) \frac{Y^4}{R^6} R_{3d}^2(r) \quad \dots (10.15a)$$

$$\langle {}^4T_{1g}(P) | \hat{V}_{A_1} | {}^4T_{1g}(P) \rangle = \left(\frac{1}{54\pi} \sqrt{\frac{5}{2}} + \frac{2}{189\pi} \sqrt{\frac{5}{2}} \right) \frac{Y^4}{R^6} R_{3d}^2(r) \quad \dots (10.15b)$$

$$\langle {}^4T_{1g}(P) | \hat{V}_{Eg} | {}^4T_{1g}(P) \rangle = \left(\frac{20}{189\pi} \frac{Y^2}{R^4} + \frac{5}{189\pi} \left(2 - \frac{\sqrt{3}}{2} \right) \frac{Y^4}{R^6} \right) R_{3d}^2(r) \quad \dots (10.15c)$$

$$\langle {}^4T_{1g}(P) | \hat{V}_{T_{2g}} | {}^4T_{1g}(P) \rangle = \left(\frac{1}{16\pi} \sqrt{\frac{2}{3}} \frac{Y^2}{R^4} + \frac{110}{3024\pi} \sqrt{\frac{2}{3}} \frac{Y^4}{R^6} \right) R_{3d}^2(r) \quad \dots (10.15d)$$

$$\langle {}^4T_{1g}(F) | \hat{V}_{A_1} | {}^4T_{1g}(F) \rangle = \left(\frac{1}{54\pi} \sqrt{\frac{5}{2}} + \frac{2}{189\pi} \sqrt{\frac{5}{2}} \right) \frac{Y^4}{R^6} R_{3d}^2(r) \quad \dots (10.15e)$$

$$\langle {}^4T_{1g}(F) | \hat{V}_{Eg} | {}^4T_{1g}(F) \rangle = \left(\left(-\frac{4}{21\pi} \sqrt{\frac{2}{3}} \frac{Y^2}{R^4} - \left(\frac{5}{54\pi} - \frac{10\sqrt{3}}{189\pi} \right) \frac{Y^4}{R^6} \right) R_{3d}^2(r) \right) \quad \dots (10.15f)$$

$$\langle {}^4T_{1g}(F) | \hat{V}_{T_{2g}} | {}^4T_{1g}(F) \rangle = \left(\frac{1}{16\pi} \sqrt{\frac{2}{3}} \frac{Y^2}{R^4} + \frac{110}{3024\pi} \sqrt{\frac{2}{3}} \frac{Y^4}{R^6} \right) R_{3d}^2(r) \quad \dots (10.15g)$$

Using the Wigner - Eckarts theorem [29]

$$\langle \Gamma_1 \chi_1 | \hat{V}_{FF} | \Gamma_2 \chi_2 \rangle = \frac{1}{\sqrt{g(\Gamma_1)}} \|\hat{V}_F\| \langle \Gamma_1 \chi_1 \Gamma_2 \chi_2 | \bar{\Gamma} \bar{\chi} \rangle \quad \dots (10.16)$$

where $\|\hat{V}_F\|$ are the reduced matrix elements of the operator

\hat{V}_{FF} which do not depend on χ , $g(\Gamma_1)$ is the dimension of

irreducible representation of the electronic state and

$\langle \Gamma_1 \chi_1 \Gamma_2 \chi_2 | \bar{\Gamma} \bar{\chi} \rangle$ are the Clebsch-Gordon coefficients [29], the

expressions for the reduced matrix elements $\|V_f\|$ are obtained as follows:

For ${}^4A_{2g} \rightarrow {}^4T_{1g}$ (P) transition,

$$\|\tilde{V}_{A_1}\| = 37/10 Dq/R \dots\dots\dots (10.17a)$$

$$\|\tilde{V}_E\| = [5/7(\sqrt{3}/2 - 2) - 20/7 \mu] Dq/R \dots\dots\dots (10.17b)$$

$$\|V_{T_2}\| = [5/2 \sqrt{3} \mu - 55/56 \sqrt{3}] Dq/R \dots\dots\dots (10.17c)$$

For ${}^4A_{2g} \rightarrow {}^4T_{1g}$ (4F) transition,

$$\|\tilde{V}_{A_1}\| = 47/10 Dq/R \dots\dots\dots (10.17d)$$

$$\|V_E\| = [-36/7 \sqrt{3} \mu + (5/2 + 10\sqrt{3}/7)] Dq/R \dots\dots\dots (10.17e)$$

$$\|V_{T_2}\| = [5/2 \sqrt{3} \mu - 55/56 \sqrt{3}] Dq/R \dots\dots\dots (10.17f)$$

where Dq is the crystal field parameter expressing the nature of the metal-ligand interaction in so far as it affects the spectral splitting. For a cubic system of O_h symmetry with MX_8 configuration it is given by

$$Dq(MX_8) = -4/27 \frac{ee^*}{R^5} \langle r^4 \rangle \dots\dots\dots (10.18)$$

and μ is a parameter given as

$$\mu = \frac{\langle r^2 \rangle}{\langle r^4 \rangle} R^2$$

where

$$\langle r^n \rangle = \int r^{n+2} R_{3d}^2(r) dr$$

$R_{3d}(r)$ is the radial function for d-electron and n is an integer.

In eq. (10.17), $\|\tilde{V}_{A_1}\|$ have been calculated by renormalizing the electron-phonon interaction operator such that

$$\langle {}^4\bar{T}_1(F) | \tilde{V}_{A_1} | {}^4\bar{T}_1(F) \rangle = \langle {}^4\bar{T}_1(F) | \hat{V}_{A_1} | {}^4\bar{T}_1(F) \rangle - \langle {}^4A_2 | \hat{V}_{A_1} | {}^4A_2 \rangle \dots (10.19a)$$

and

$$\langle {}^4\bar{T}_1(P) | \tilde{V}_{A_1} | {}^4\bar{T}_1(P) \rangle = \langle {}^4\bar{T}_1(P) | \hat{V}_{A_1} | {}^4\bar{T}_1(P) \rangle - \langle {}^4A_2 | \hat{V}_{A_1} | {}^4A_2 \rangle \dots (10.19b)$$

In this expressions, Dq and R are known while the parameter μ can be calculated using the radial wavefunction of free ions.

11. The phonon sums

The determination of the Van-Vleck coefficients $\vec{a}_{22}(F\bar{r})$ eq. (7.10) and the quantities $b_{22\nu}(F\bar{r})$ eq. (7.13) will be restricted to the approximate sums in the "Extended Brillouin Zone" scheme as was mentioned earlier. In the "Extended Brillouin Zone" scheme, the phonon sum for the accoustical mode of vibration is calculated in Debye's model with a cut off wave vector : $\omega_D = (6\pi^2/V_0)^{1/3}$ which extends beyond the boundary of the first Brillouin Zone, where V_0 is the volume of unit primitive cell. For the optical mode of vibration, the Einstein model is applied. This is because the polarization vector $\vec{e}(\omega\nu)$ for all directions in the Brillouin Zone for all branches of lattice vibrations are not available in the literature and therefore could not be used. However, the experimental determination of dispersion

relations for phonon frequency against the phonon wave vector for $\text{CdF}_2:\text{Co}^{2+}$ and $\text{CaF}_2:\text{Co}^{2+}$ have been carried out by [34]. The frequency of the longitudinal optical mode obtained by the above mentioned was relatively high as determined from the analysis of reflection spectrum. Pamela et. al. [34] attributes this discrepancy to the difficulties encountered in preparing thin films of ideal crystal structure and thickness.

Now, the Van-Vleck coefficients $\vec{A}_{\vec{x}\nu}$, and the quantities $b_{\vec{x}\nu}$ will be calculated in the case of the "Extended Brillouin Zone" scheme in which real coordinates, real polarization vector and Van-Vleck coefficients can be used. The required Van-Vleck coefficients transform in the same way as the bases of the T_{2g} , E_g and A_{1g} Irreducible Representation (IR). Since the bases of the T_{2g} - IR are not real [29] a unitary transformation is applied to make them real within the sub-space belonging to the T_{2g} IR. It is possible to do so because any unitary transformation within a degenerate sub-space does not affect any physical situation. Therefore, $\exp[-i \vec{x} \cdot R_{0\alpha}]$ in eq. (7.10) is replaced by $2 \sin[\vec{x} \cdot \vec{R}_\alpha + \pi/4]$. For the impurity centre of O_h symmetry, the Van-Vleck coefficients are [35].

$$\vec{A}_{\vec{x}\nu}(A_{1g}) = \frac{2}{\sqrt{6}} \sin \pi/4 (\vec{E}_x \sin \vec{x}_x R_0 + \vec{E}_y \sin \vec{x}_y R_0 + \vec{E}_z \sin \vec{x}_z R_0) \dots\dots (11.1a)$$

$$\vec{A}_{\vec{x}\nu}(E_u) = \frac{1}{\sqrt{3}} \sin \pi/4 (\vec{E}_x \sin \vec{x}_x R_0 + \vec{E}_y \sin \vec{x}_y R_0 - 2\vec{E}_z \sin \vec{x}_z R_0) \dots\dots (11.1b)$$

$$\vec{A}_{\vec{x}\nu}(\bar{E}\nu) = \sin \pi/4 (\vec{e}_x \sin \vec{x}_x R_0 - \vec{e}_y \sin \vec{x}_y R_0) \dots (11.1c)$$

$$\vec{A}_{\vec{x}\nu}(\bar{T}_{2g}) = \sin \pi/4 (\vec{e}_z \sin \vec{x}_y R_0 + \vec{e}_y \sin \vec{x}_z R_0) \dots (11.1d)$$

$$\vec{A}_{\vec{x}\nu}(\bar{T}_{2g}) = \sin \pi/4 (\vec{e}_x \sin \vec{x}_z R_0 + \vec{e}_z \sin \vec{x}_x R_0) \dots (11.1e)$$

$$\vec{A}_{\vec{x}\nu}(\bar{T}_{2g}) = \sin \pi/4 (\vec{e}_y \sin \vec{x}_x R_0 + \vec{e}_x \sin \vec{x}_y R_0) \dots (11.1f)$$

To determine $b_{\vec{x}\nu}$, the polarization vector $\vec{e}_{\vec{x}\nu}$ is expanded in the directions parallel and perpendicular to the phonon wavevector \vec{x} (see fig. 11). From fig. 11, when $\vec{e} \parallel \vec{x}$ then

$$e_x = \sin \theta \cos \varphi = \frac{\vec{x}_x}{x} \dots (11.2a)$$

$$e_y = \sin \theta \sin \varphi = \frac{\vec{x}_y}{x} \dots (11.2b)$$

$$e_z = \cos \theta = \frac{\vec{x}_z}{x} \dots (11.2c)$$

When $\vec{e} \perp \vec{x}$ then,

$$e_x = \cos \varphi \cos \varphi + \sin \varphi \cos \varphi \dots (11.3a)$$

$$e_y = \cos \varphi \sin \varphi \cos \theta - \sin \varphi \cos \varphi \dots (11.3b)$$

$$e_z = -\cos \varphi \sin \theta \dots (11.3c)$$

and

$$\vec{x}_x R = x R \sin \theta \cos \varphi \dots (11.4a)$$

$$\vec{x}_y R = x R \sin \theta \sin \varphi \dots (11.4b)$$

$$\vec{x}_z R = x R \cos \theta \dots (11.4c)$$

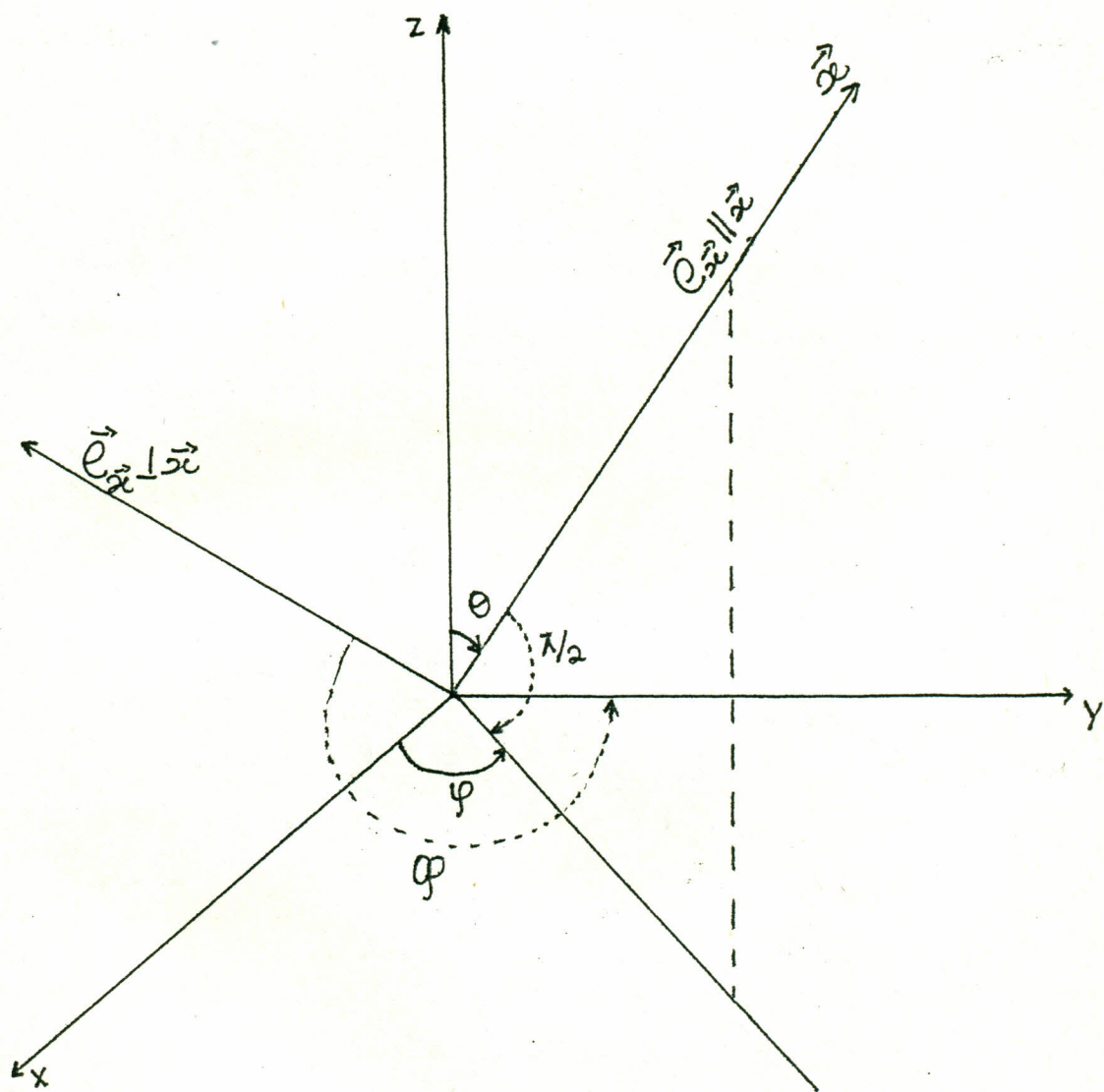


Fig. 11. The polar coordinates of the polarization vector

$\vec{e}_{\vec{x}}$.

with

$$0 \leq \theta \leq \pi \quad 0 \leq \varphi \leq 2\pi \quad 0 \leq \varphi' \leq 2\pi$$

Taking the integration and averaging over the squares of Van-Vleck coefficients, the following expressions for $b_{\xi L}(\bar{r})$ are obtained

$$b_{\xi L}(A_1) = \frac{1}{6} - \frac{\sin 2\xi}{4\xi} + \frac{\sin 2\xi}{8\xi^3} - \frac{\cos 2\xi}{4\xi^2} - \frac{\sin \sqrt{2}\xi}{\sqrt{2}\xi} + \frac{3\sin \sqrt{2}\xi}{2\sqrt{2}\xi^3} - \frac{3\cos \sqrt{2}\xi}{2\xi^2} \dots (11.5a)$$

$$b_{\xi t}(A_1) = \frac{1}{6} - \frac{\sin 2\xi}{16\xi^3} + \frac{\cos 2\xi}{8\xi^2} + \frac{\sin \sqrt{2}\xi}{2\sqrt{2}\xi} - \frac{3\sin \sqrt{2}\xi}{4\sqrt{2}\xi^3} + \frac{3\cos \sqrt{2}\xi}{4\xi^2} \dots (11.5b)$$

$$b_{\xi L}(E) = \frac{1}{6} - \frac{\sin 2\xi}{4\xi} + \frac{\sin 2\xi}{8\xi^3} - \frac{\cos 2\xi}{4\xi^2} + \frac{\sin \sqrt{2}\xi}{2\sqrt{2}\xi} - \frac{3\sin \sqrt{2}\xi}{4\sqrt{2}\xi^3} + \frac{3\cos \sqrt{2}\xi}{4\xi^2} \dots (11.5c)$$

$$b_{\xi t}(E) = \frac{1}{6} - \frac{\sin 2\xi}{16\xi^3} + \frac{\cos 2\xi}{8\xi^2} - \frac{\sin \sqrt{2}\xi}{4\sqrt{2}\xi} + \frac{3\sin \sqrt{2}\xi}{8\sqrt{2}\xi^3} - \frac{3\cos \sqrt{2}\xi}{8\xi^2} \dots (11.5d)$$

$$b_{\xi L}(T_2) = \frac{1}{6} - \frac{\sin 2\xi}{16\xi^3} + \frac{\cos 2\xi}{8\xi^2} - \frac{\sin \sqrt{2}\xi}{2\sqrt{2}\xi} + \frac{3\sin \sqrt{2}\xi}{4\sqrt{2}\xi^3} - \frac{3\cos \sqrt{2}\xi}{4\xi^2} \dots (11.5e)$$

$$b_{\xi t}(T_2) = \frac{1}{6} - \frac{\sin 2\xi}{8\xi} + \frac{\sin 2\xi}{32\xi^3} - \frac{\cos 2\xi}{16\xi^2} + \frac{\sin \sqrt{2}\xi}{4\sqrt{2}\xi} - \frac{3\sin \sqrt{2}\xi}{8\sqrt{2}\xi^3} + \frac{3\cos \sqrt{2}\xi}{8\xi^2} \dots (11.5f)$$

In the above expressions $\xi = \alpha R_0$ is a dimensionless coordinate.

To carry out the calculations, for the second and third moments, the expressions for these moments eqs. (8.8) and (8.14) are to be expressed in integral form. First, the Wigner-Eckarts theorem in matrix form is applied to the operator such that

$$\hat{V}_{\bar{f}\bar{f}} = \frac{1}{\sqrt{g(f)}} \parallel \hat{V}_{\bar{f}} \parallel \hat{O}_{\bar{f}\bar{f}} \quad \dots\dots\dots (11.6)$$

where $\parallel \hat{V}_{\bar{f}} \parallel$ is the reduced matrix element which is independent of the index of the row \bar{f} of irreducible representation \bar{f} . $\hat{O}_{\bar{f}\bar{f}}$ are the Clebsh-Gordon coefficients matrix which satisfies the orthogonality relation

$$\sum_{\bar{f}} \hat{O}_{\bar{f}\bar{f}}^+ \hat{O}_{\bar{f}\bar{f}} = \hat{1} \quad \dots\dots\dots (11.7)$$

Now, changing the summation in eq. (8.8) to integration with respect to α and using the Wigner-Eckarts theorem, the expression for the second moment (\hat{O}_2) becomes

$$\hat{O}_2 = \frac{1}{2\hbar M} \frac{L^3}{(2\pi)^3} \sum_{F\nu} \frac{1}{g(F)} \parallel \hat{V}_{\bar{f}} \parallel^2 \int_0^{\alpha_0} \frac{\alpha^2 b_{\alpha\nu}(F)}{\omega_{\alpha\nu}} \coth \frac{B_{\alpha\nu}}{2} d\alpha \quad \dots (11.8)$$

where α_0 is Debye cut off phonon wavevector.

Changing the valuable α to dimension less variable ξ and applying the Debye dispersion relation for accoustical mode of vibration i.e $\omega_{\alpha\nu} = \alpha v_s$ and the Einstein relation for optical modes of

vibration (ie optical frequency ω_0 assumed to be independent of \vec{x}), the following expression in integral form is obtained for the second moment

$$\hat{G}_2 = \frac{1}{16\pi^3 \rho \hbar g(F) R_0^2} \sum_F \|\hat{V}_F\|^2 \int_0^{\xi_D} \xi^2 d\xi \left[\frac{b_{\xi L}^{(F)}}{\xi v_L} \coth \frac{\hbar v_L \xi}{2R_0 k_B T} + \frac{2b_{\xi t}^{(F)}}{\xi v_L} \coth \frac{\hbar v_L \xi}{2R_0 k_B T} + \frac{b_{\xi L}^{(F)}}{\omega_{0L} R_0} \coth \frac{\hbar \omega_{0L}}{2k_B T} + \frac{2b_{\xi t}^{(F)}}{\omega_{0L} R_0} \coth \frac{\hbar \omega_{0L}}{2k_B T} \right] \dots (11.9)$$

where $\xi_D = \alpha_D R = \sqrt{3}/2 a_0 \alpha_D$ and a_0 is the crystal lattice constant. The perturbation independent part of the third moment is given by eq. (8.14). Using the same argument as above and taking into account one longitudinal and two transverse modes for both optical and accoustical branches, the final expression for the third moment is obtained as follows

$$\hat{G}_3 = \frac{1}{8\pi^3 R_0^3 \rho \hbar g(F)} \sum_F \|\hat{V}_F\|^2 \int_0^{\xi_D} \xi^2 d\xi (b_{\xi L}^{(F)} + 2b_{\xi t}^{(F)}) \dots (11.10)$$

where ρ is the density of the crystal.

i) The Jahn-Teller stabilization energy

Let \hat{H}_Y be the diagonal matrix element between the electronic states $|r\gamma\rangle$ of the total Hamiltonian given by eq. (1.1). Then in terms of the creation $\hat{C}_{\vec{x}\nu}^+$ and annihilation $\hat{C}_{\vec{x}\nu}$ operators \hat{H}_Y can be written as

$$\hat{H}_Y = \langle r\gamma | \hat{H} | r\gamma \rangle = \langle r\gamma | \hat{H}_e | r\gamma \rangle + \sum_{\vec{x}} (v_{\vec{x}\nu} \hat{C}_{\vec{x}}^+ + v_{\vec{x}\nu}^* \hat{C}_{\vec{x}\nu}) + \sum_{\vec{x}} \hbar \omega_{\vec{x}} \hat{C}_{\vec{x}}^+ \hat{C}_{\vec{x}} \dots (11.11)$$

where $V_{\vec{x}}^e = \langle r\delta | V_{\vec{x}}^{(ad)} | r\delta \rangle$ and $V_{\vec{x}}^{(ad)}$ implies that the non-adiabatic part of the interaction Hamiltonian \hat{H}_{e1} is neglected.

Noting that neither are $|r\delta\rangle$ exact eigenfunctions nor $\langle r\delta | \hat{H}_e | r\delta \rangle = E_r$ exact eigenvalues of the Hamiltonian \hat{H}_e , and making use of suitable mathematical formalism for perturbation theory based on unitary transformation, \hat{H}_y can be transformed as

$$\tilde{H}_y = e^{-S} \hat{H}_y e^S \quad \dots\dots (11.12)$$

where S is anti-Hermitian operator which takes the form

$$\hat{S} = \sum_{\vec{x}\nu} (P_{\vec{x}}^{(\delta)} C_{\vec{x}\nu}^+ - P_{\vec{x}}^{(\delta)*} C_{\vec{x}\nu}) \quad \dots\dots (11.13)$$

Here, \hat{H}_y is taken as an operator acting in the phonon subspace. The values of $P_{\vec{x}}^{(\delta)}$ can be determined by expanding

$$\tilde{H}_y = \hat{H}_y + [\hat{H}_y, \hat{S}] + \frac{1}{2} \{[\hat{H}_y, \hat{S}], \hat{S}\} + \dots\dots (11.14)$$

and since the linear terms in S vanish in the expansion, eq. (11.14), that is

$$[\hat{H}_y, \hat{S}] + \hat{H}_{e1} = 0 \quad \dots\dots\dots (11.15)$$

then

$$P_{\vec{x}}^{(\delta)} = -V_{\vec{x}\nu}^e / \hbar \omega_{\vec{x}\nu} \quad \dots\dots (11.16)$$

In this approximation the second-order Hamiltonian \hat{H}_y is obtained

as

$$\hat{H}_Y = \langle r_Y | \hat{H}_e | r_Y \rangle - \sum_{\alpha} \frac{|\langle r_Y | V_{\alpha}^{(Y)} | r_Y \rangle|^2}{\hbar \omega_{\alpha}} + \sum_{\alpha} \hbar \omega_{\alpha} C_{\alpha}^+ C_{\alpha} \dots (11.17)$$

where the second term in eq. (11.17) is called the Jahn-Teller stabilization energy (ΔE^{J-T}).

Expressing $V_{\alpha}^{(Y)}$ in terms of irreducible tensor operator $\hat{V}_{F\bar{F}}$ and using the Wigner-Eckarts theorem, the expression for Jahn-Teller stabilization energy is obtained as follows

$$\Delta E^{J-T} = \frac{g(F)}{2M\hbar} \sum_{\alpha} \sum_{\bar{F}} \frac{b_{\alpha\nu}^{(F)}}{\omega_{\alpha\nu}^2} \|\dot{V}_{\bar{F}}\|^2 \dots (11.18)$$

which can be expressed in integral form as

$$\Delta E^{J-T} = \frac{1}{2M\hbar} \frac{L^3}{(2\pi)^3} g(F) \sum_{\bar{F}} \|\dot{V}_{\bar{F}}\|^2 \int_0^{\alpha_0} \frac{\alpha^2 b_{\alpha\nu}^{(F)}}{\omega_{\alpha\nu}} d\alpha \dots (11.19)$$

Applying the Debye's and Einsteins approximation for lattice vibrations as was done for second and third moments and changing the variable α to dimensionless variable ξ , the expression for the Jahn-Teller stabilization energy becomes

$$\Delta E^{J-T} = \frac{1}{16\pi^3 \rho \hbar R_0 g(F)} \sum_{\bar{F}} \|\dot{V}_{\bar{F}}\|^2 \int_0^{\xi_0} \xi^2 d\xi \times \left[\frac{b_{\xi l}(F)}{\xi^2 V_c^2} + \frac{2b_{\xi t}(F)}{\xi^2 V_c^2} + \frac{b_{\xi l}(F)}{\omega_{0l}^2 R_0^2} + \frac{2b_{\xi t}(F)}{\omega_{0l}^2 R_0^2} \right] \dots (11.20)$$

In the calculations of the moments and Jahn-Teller stabilization energy, the following phonon parameters were used (Table 3)

TABLE 3. Phonon Parameters [34]

	CdF ₂	CaF ₂
Density, (ρ) kgm ⁻³	6.33 x 10 ³	3.18 x 10 ³
Lattice Constant x 10 ⁻¹⁰ m	5.388	5.463
Nearest neighbour distance x 10 ⁻¹⁰ m	4.666	4.73
Longitudinal velocity of sound (V_L) - ms ⁻¹	4521	6858
Transverse velocity of sound (V_t) ms ⁻¹	2863	3960
Longitudinal optical phonon frequency $\omega_{ol}(s^{-1})$	6.028 x 10 ¹³	6.38 x 10 ¹³
Transverse, optical phonon frequency $\omega_{ot}(s^{-1})$	6.028 x 10 ¹³	6.38 x 10 ¹³

The third moment (σ_3) is known to determine the asymmetry of the band shape. The asymmetry deviation of the band shape from the Gaussian form can be described by the third coefficient (γ_3) of Edgeworth series defined as [18].

$$\gamma_3 = \frac{\langle \sigma_3 \rangle}{\langle \sigma_2 \rangle^{3/2}} \dots\dots\dots (11.21)$$

For strong electron-phonon interaction, $\gamma_3 \ll 1$, a condition that indicate the presence of strong Jahn-Teller lattice vibrations.

ii) Comparison of theoretical and experimental values of the Jahn-Teller Electron-Phonon Interaction parameters

The second and third moments of the absorption bands of Co^{2+} in CdF_2 and CaF_2 arising from the ${}^4A_{2g} \longrightarrow {}^4T_{1g}(\text{P})$ and ${}^4A_{2g} \longrightarrow {}^4T_{1g}(\text{F})$ transitions have been calculated at 78K using eqs. (11.9) and (11.10). The Jahn-Teller stabilization energy ($\Delta E^{\text{J-T}}$) and the third coefficient (σ_3) of Edgeworth series have also been computed using eq. (11.20) and eq. (10.21) respectively. Both experimental and theoretical results appear in Table 4. The temperature dependence of the second moment for ${}^4A_{2g} \longrightarrow {}^4T_{1g}(\text{P})$ and ${}^4A_{2g} \longrightarrow {}^4T_{1g}(\text{F})$ transitions are shown in fig. 12 for $\text{CdF}_2:\text{Co}^{2+}$ and in fig. 13 for $\text{CaF}_2:\text{Co}^{2+}$.

iii) Energy separation (ΔE) between extreme peaks

The half band width of the non-Gaussian curve is given by [37].

$$\Delta \Omega = \frac{\sigma_3}{\sigma_2} \left[1 + \frac{8\sigma_2^3}{\sigma_3^2} \ln \left(\frac{2}{1 - \frac{3\sigma_3^2}{8\sigma_2^3}} \right) \right]^{\frac{1}{2}} \dots\dots (11.22)$$

Experimentally, in place of this half band width, the energy separation (ΔE) between the extreme peaks (see fig. 14) has been determined [31, 33]. To compare these two values an experimental fit has been taken at 300K. This mathematical reduction factor α is not a bad approximation since the extreme peaks are nearly symmetrical about the central peak (fig. 3 and 4). This factor is defined as

$$\alpha = \frac{\Delta E}{\Delta \Omega} \dots\dots\dots (11.23)$$

and has been calculated at 300K.

TABLE 4. Jahn-Teller Electron-Phonon Interaction parameters

		CdF ₂ :Co ²⁺		CaF ₂ :Co ²⁺	
		⁴ A ₂ → ⁴ T _{1(P)}	⁴ A ₂ → ⁴ T _{1(F)}	⁴ A ₂ → ⁴ T _{1(P)}	⁴ A ₂ → ⁴ T _{1(F)}
G ₂ (78k) x 10 ⁻³ (eV ²)	Theor.	8.9	14.3	12.1	19.7
	Expt.	[38] 9.6	- -	[38] 10.2	- -
G ₃ (78k) x 10 ⁻⁴ (eV ³)	Theor.	1.51	2.44	3.00	4.85
	Expt.	[38] 3.12	- -	[38] 2.86	- -
ΔE ^{J-T} (eV)	Theor.	0.196	0.30	0.181	0.292
	Expt.	[31] 0.23	[31] 0.26	[32] 0.223	[32] 0.248
Y ₃ (78k)	Theor.	0.018	0.014	0.022	0.017

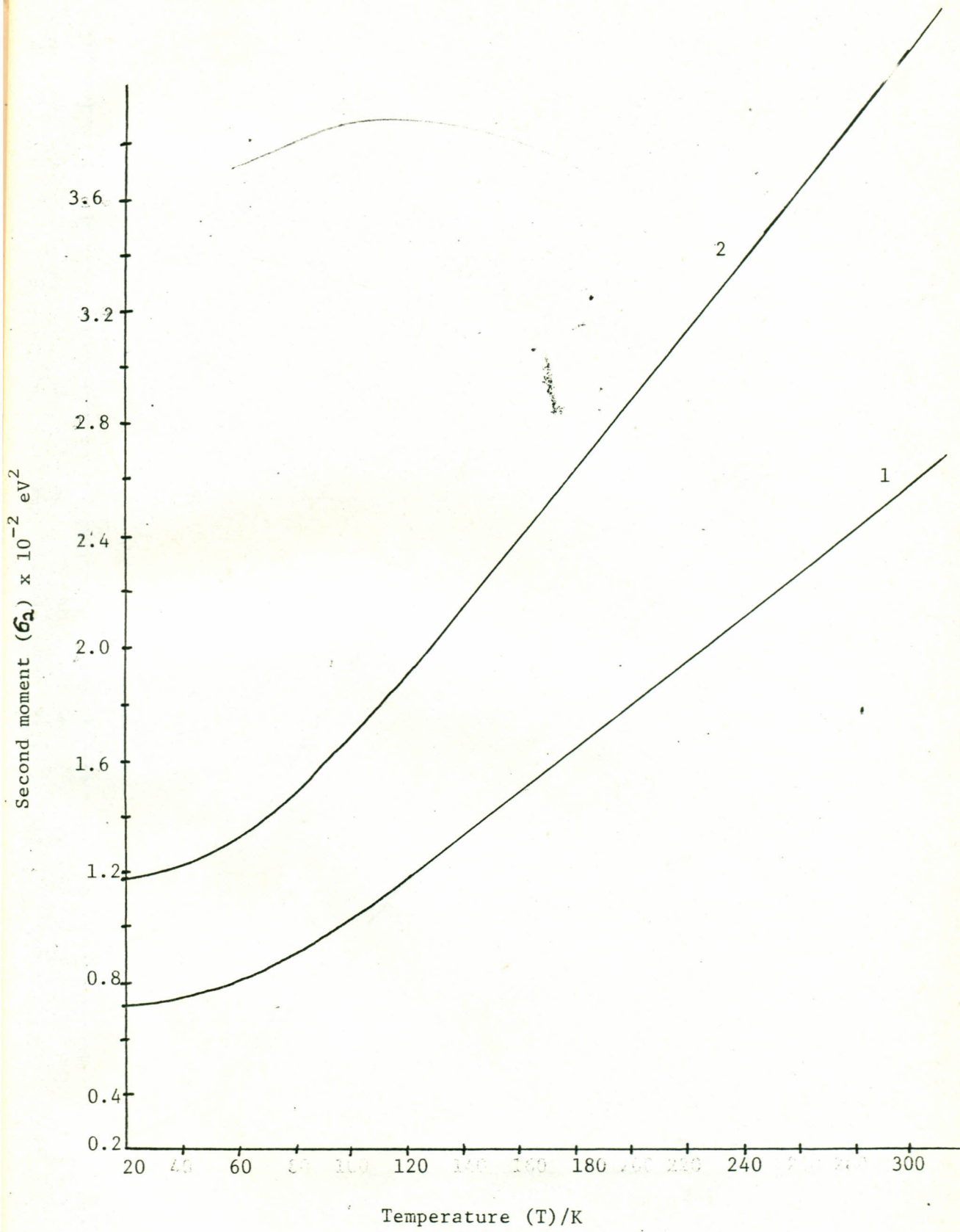


Fig. 12. Temperature dependence of second moments of (1) ${}^4T_{1g} \rightarrow {}^4T_{1g}(P)$
(2) ${}^4A_{2g} \rightarrow {}^4T_{1g}(F)$ absorption bands of Co^{2+} in CdF_2 .

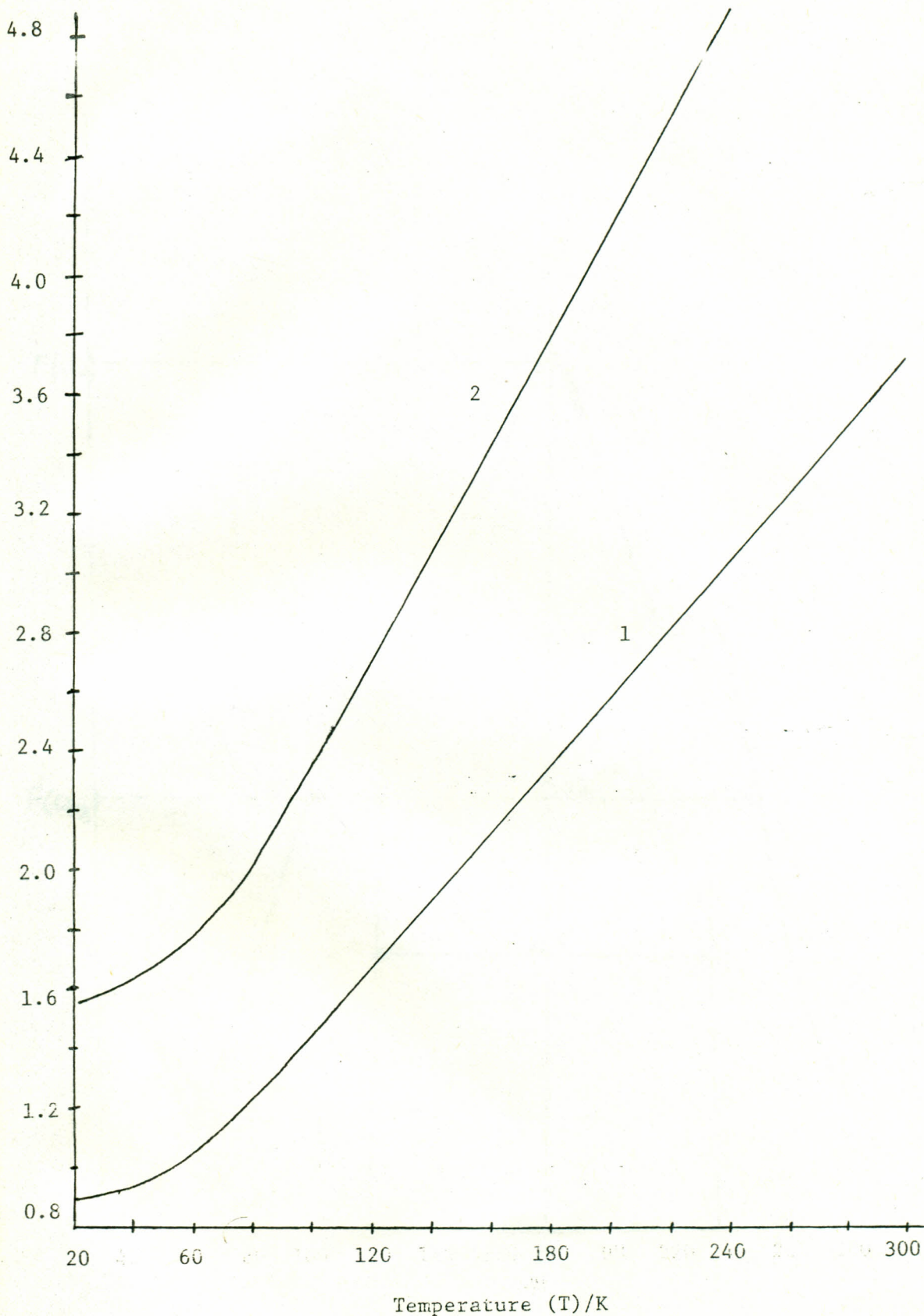


Fig. 13. Temperature dependence of second moments of
(1) ${}^4A_{2g} \rightarrow {}^4T_{1g}(P)$, (2) ${}^4A_{2g} \rightarrow {}^4T_{1g}(F)$ absorption
bands of Co^{2+} in CaF_2 .

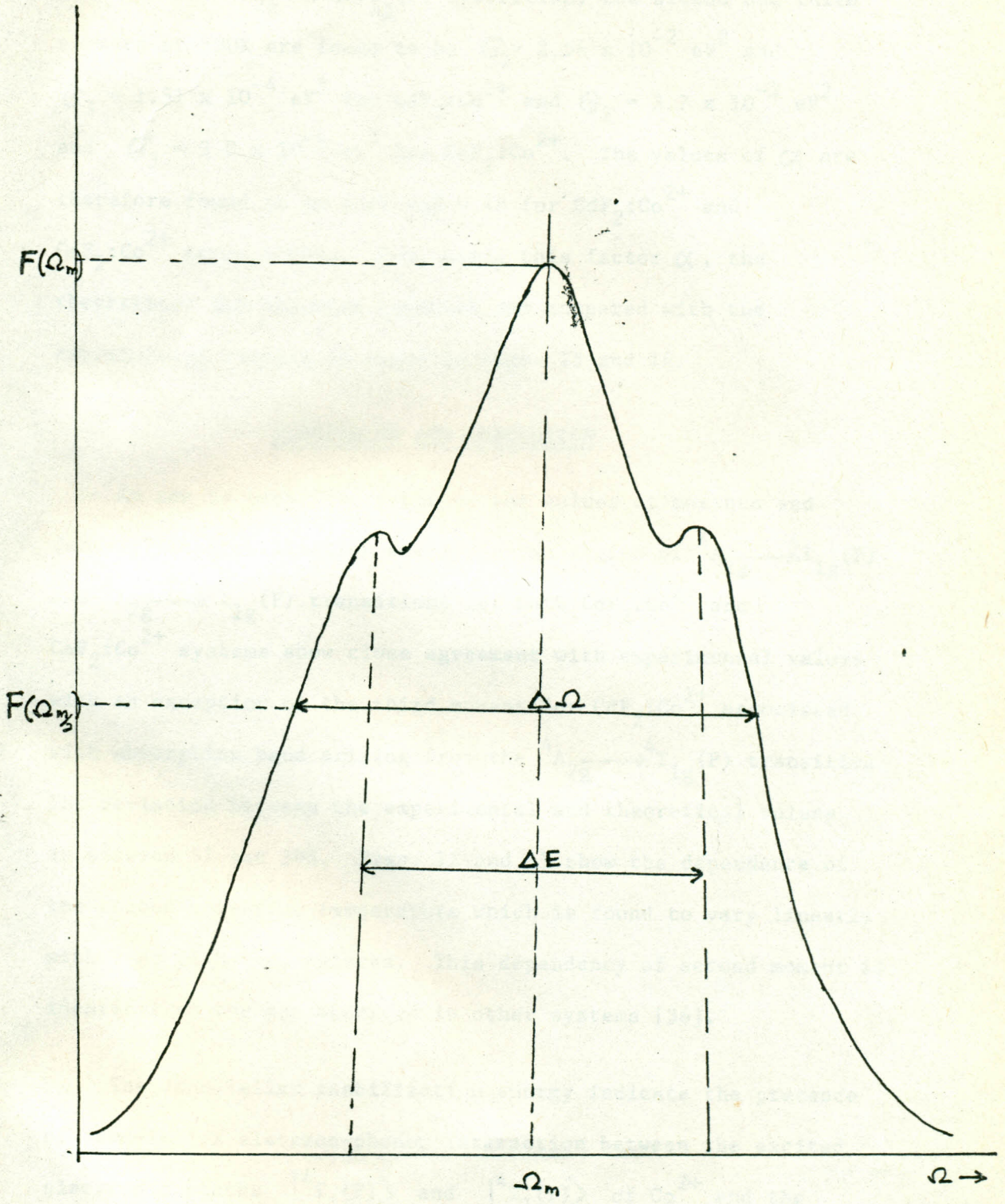


Fig. 14. Optical absorption spectra.

For the ${}^4A_{2g} \rightarrow {}^4T_{1g}$ (P) transition, the second and third moments at 300K are found to be $G_2 = 2.56 \times 10^{-2} \text{ eV}^2$ and $G_3 = 1.51 \times 10^{-4} \text{ eV}^3$ for $\text{CdF}_2:\text{Co}^{2+}$ and $G_2 = 3.7 \times 10^{-2} \text{ eV}^2$ and $G_3 = 3.0 \times 10^{-4} \text{ eV}^3$ for $\text{CaF}_2:\text{Co}^{2+}$. The values of α are therefore found to be 0.67 and 0.48 for $\text{CdF}_2:\text{Co}^{2+}$ and $\text{CaF}_2:\text{Co}^{2+}$ respectively. Now, using this factor α , the theoretical ΔE has been computed and compared with the experimental results as shown in figs. 15 and 16.

DISCUSSION AND CONCLUSION

As can be seen from table 4, the values of moments and Jahn-Teller stabilization energy in the region of ${}^4A_{2g} \rightarrow {}^4T_{1g}$ (P) and ${}^4A_{2g} \rightarrow {}^4T_{1g}$ (F) transitions for both $\text{CdF}_2:\text{Co}^{2+}$ and $\text{CaF}_2:\text{Co}^{2+}$ systems show close agreement with experimental values with an exception of the third moment for $\text{CdF}_2:\text{Co}^{2+}$ associated with absorption band arising from the ${}^4A_{2g} \rightarrow {}^4T_{1g}$ (P) transition. The deviation between the experimental and theoretical values is between 5% and 50%. Figs. 12 and 13 show the dependence of the second moment on temperature which is found to vary linearly with T at high temperatures. This dependency of second moment is identical to the one observed in other systems [36].

The Jahn-Teller stabilization energy indicate the presence of Jahn-Teller electron-phonon interaction between the excited electronic states $|{}^4T_1(\text{P})\rangle$ and $|{}^4T_1(\text{F})\rangle$ of Co^{2+} and the lattice vibrations of the ligands. Since $\Delta E^{\text{J-T}}({}^4\text{P}) > \Delta E^{\text{J-T}}({}^4\text{F})$ there is a stronger electron-phonon interaction for the $|{}^4\text{F}\rangle$ electronic state than for the $|{}^4\text{P}\rangle$ state. Further, it is seen from table 4 that for both the transitions ${}^4A_{2g} \rightarrow {}^4T_{1g}$ (P)

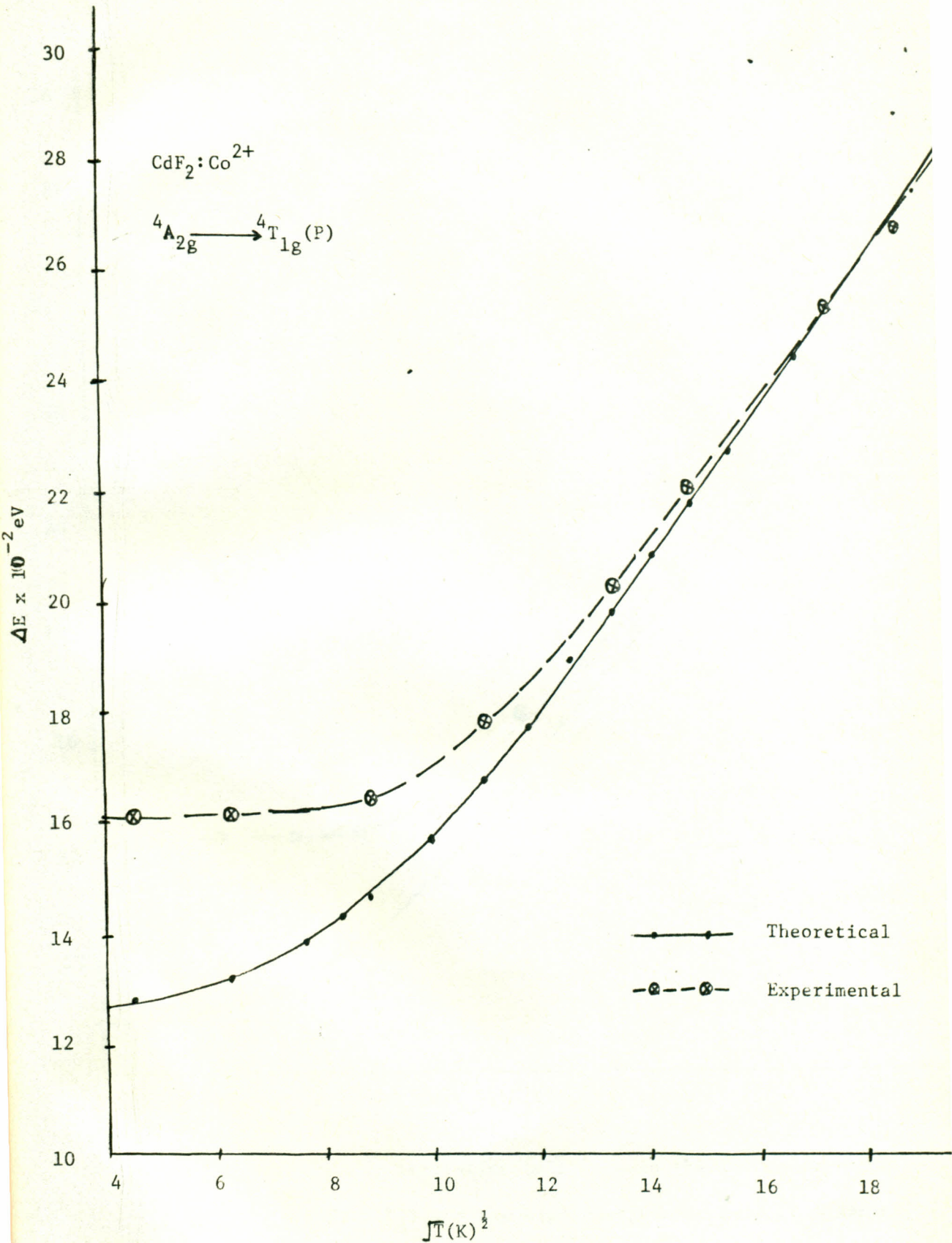


Fig. 15. Energy separation (ΔE) between the low energy side peak (E_L) and the high energy side peak (E_h) for the ${}^4\text{A}_{2g} \longrightarrow {}^4\text{T}_{1g}(\text{P})$ transition against \sqrt{T} .

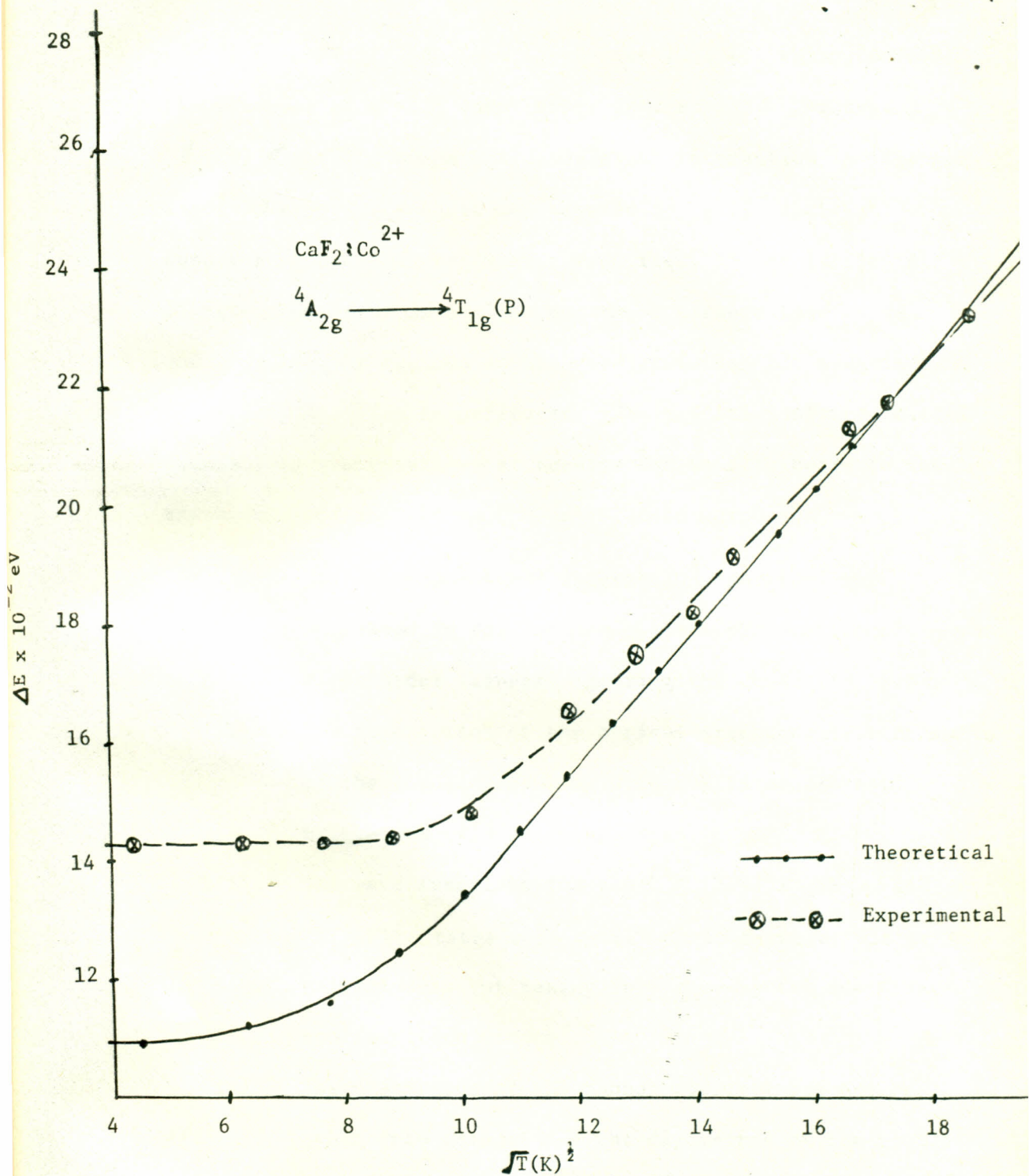


Fig. 16. Energy separation (ΔE) between the low energy side peak (E_l) and the high energy side peak (E_h) for the ${}^4\text{A}_{2g} \longrightarrow {}^4\text{T}_{1g}(\text{P})$ transition against \sqrt{T} .

and ${}^4A_{2g} \longrightarrow {}^4T_{1g}(F)$ in both the systems, $\gamma_3 \ll 1$ which indicates the presence of strong Jahn-Teller interaction. Moreover,

$\gamma_3({}^4F) < \gamma_3({}^4P)$, hence the Jahn-Teller interaction is stronger for $|{}^4F\rangle$ electronic state as compared to $|{}^4P\rangle$ state which supports our earlier argument. From figs. 15 and 16, it is evident that there is a close agreement between theoretical and experimental results at high temperatures, but a deviation of about 20% at low temperatures. The deviation of theoretical values from the experimental results can be attributed to the approximations applied in the calculation which are,

- i) The electron-phonon interaction operators were expressed in the lattice-point approximation of first order (linear) ignoring the quadratic terms.'
- ii) The interaction of the optical electrons (electrons of the impurity centre) with the first nearest neighbours only was considered.
- iii) The wave functions for the $|{}^4A_{2g}\rangle$, $|{}^4T_{1g}(P)\rangle$ and $|{}^4T_{1g}(F)\rangle$ states were expressed in terms of Slater determinants but taking into account the electron configuration mixing.
- iv) The dispersion of the phonon spectrum has not been taken into account i.e the dependence of the phonon frequency on the wavevector \vec{k} has been ignored.
- v) The phonon sum appearing in the expressions for the second moment and Jahn-Teller stabilization energy, has been determined in the "Extended Brillouin Zone" scheme with extended cut off wave vector, α_0 ,

In conclusion, the lattice-point model for electron-phonon interaction and the "Extended Brillouin Zone" scheme to the phonon sum prove valid to absorption spectra by d-electron impurity centres in crystals with cubic symmetry and in particular to the $\text{CdF}_2:\text{Co}^{2+}$ and $\text{CaF}_2:\text{Co}^{2+}$ crystals. The presence of strong Jahn-Teller interaction in these activated crystals has been implied in the calculated results which have also been observed experimentally. More accurate results could be obtained if the above cited approximations are taken into account e.g considering interaction with second nearest neighbours, considering the quadratic terms in the EPI operator, the dependence of the phonon frequency on the wavevector \vec{q} etc.

REFERENCES

1. M. Lax, Journal of Phy. Chem. 20, 1752 - 1761, 1952.
2. K. Huang and A.R. Rhays, Proc. Roy. Soc. A204, 406 - 417, 1950.
3. I.B. Bersuker, The Jahn-Teller Effect and vibronic interaction in modern Chemistry, Plenum Press New York and London, 1984, pp. 1.
4. M. Wagner, Z. Physik 230, 460 - 480, 1970.
5. H.A. Jahn and E.Teller, Proc. Roy. Soc. London, A161, 220 - 235, 1937.
6. M.C.M. O'Brien, Proc. Phys. Soc. 86, 847 - 857, 1965.
7. P.R. Moran, Phys. Rev. A137, 1016 - 1027, 1965.
8. Y. Toyozawa and M. Inoue, J. Phys. Soc. Japan, 20, 1289 - 1290, 1965.
9. K. Cho., J. Phys. Soc. Japan, 25, 1372 - 1387, 1968.
10. A. Fakuda, J. Phys. Soc. Japan 27, 96 - 109, 1969.
11. L. Higgins, H.C. Opik, U. Pryce, M.H.L. Sack, Proc. Roy. Soc. London, Series A, 244, 1 - 16, 1958.
12. H. Kamimura and T. Yamaguchi, J. Phys. Soc. Japan 25, 1138 - 1147, 1968.
13. H.D. Koswig and I. Kunze, Phys. Stat. Sol. (German) 9, 451 - 461, 1965.
14. V.P. Chlopin, B.S. Tsukerblat, Yu. B. Rosenfeld, and I.B. Bersuker, Phys. Stat. Sol.(b), 52, K72 - K75 1972.
15. M. Caner and R. Englman, J. Chem. Phys. 44 4054 - 4055, 1966.
16. C.H. Henry, S.E. Schnattely, C.P. Slitcher, Phys. Rev. 137, A583 - 602, 1965.

17. A.Honma, J. Phys. Soc. Japan, 20, 1082 - 1095, 1968.
18. Yu, E. Perlin and B.S. Tsukerblat, Dynamical Jahn-Teller Effect in localized systems, Ed. Yu. E. Perlin and M. Wagner, Elsevier science publishers, B.V. 1984, pp. 253 - 346.
19. R.W.H. Stephenson, Phonons in perfect lattice and in lattice with point imperfections, Scottish Universities Summer School, Ed. T. Smith, Edinburgh and London 1965.
20. E. Merzbacher, Quantum mechanics, John Wiley and Sons, Inc. London, 1970, pp. 362 - 64.
21. J.R. Waldram, Theory of thermodynamics, Cambridge University press, Cambridge 1985, pp. 30 - 32.
22. H. Eyring, D. Henderson, B.J. Stower and E.M. Eyring, Statistical Mechanics and Dynamics, John Wiley and Sons, New York 1982.
23. M. Lax, Symmetry principles in solid state and molecular physics, John Wiley and Sons, New York 1974.
24. J.H. Van-Vleck, Phy. Rev. 57, 426 - 447, 1940.
25. Yu. E. Perlin, B.S. Tsukerblat, T.S. Dod, Phys. Stat. Sol. (b) 80, 703 - 707 1977.
26. R.E. Hetrick, Phys. Rev. 188, 1392 - 1403, 1969.
27. Y. Meile, d'Aubigne and A.Roussel, Phys. Rev. B 3, 1421 - 1424, 1971.
28. C. Escribe and A.E. Highes, J. Phys. C. 4 2537 - 2548, 1971.
29. S. Sugano, Y. Tabane, H. Kamimura, Multiplets of transition metal ions in crystals, Academic press, New York and London 1970.
30. M.N. Jones, Spherical harmonics and tensors for classical

field theory, John Wiley and Sons, Inc. New York 1985
pp. 107.

31. W. Ulrici, phys. stat. sol. (b) 62 431 - 441 1974.
32. G. Schwotzer and W. Ulrici Phys. Stat. Sol. (b) 64
K115 - 118, 1974.
33. P.J. Alonso and R. Alcala, Phys. Stat. Sol. (b) 81 333 -
339, 1977.
34. D. Pamela, G.R. Field, P.L.R. Morse and G.R. Wilkinson
Proc. Roy. Soc. London, A317, 55 - 77, 1970.
35. Yu. E. Perlin and B.S. Tsukerblat, the effects of electron
vibrational interactions in the optical spectra of the
paramagnetic impurity ions. Shtiintsa, Kishinev,
(Russian) 1974, pp. 47.
36. T.S. Dod, Proceedings of all India. Symposium on Nuclear
Physics and Solid State Physics, New Delhi 23C, 359 - 361,
1980.
37. J.F. Koga, Moments of A \longrightarrow T absorption band in activated
crystals, MSc. thesis, Kenyatta University 1987, pp. 63.
38. V.A. Krylov and W. Ulrici, phys. stat. sol. (b) 84 215 -
224, 1977.